ALPHA-DESYNCHRONIZING ELECTROENCEPHALOGRAM-NEUROFEEDBACK MODULATES POSTERIOR CINGULATE CORTEX AND PERIAQUEDUCTAL GRAY RESTING-STATE FUNCTIONAL CONNECTIVITY IN POST-TRAUMATIC STRESS DISORDER

Susan Ellen Elizabeth MacGowan

Thesis submitted to the University of Ottawa
in partial Fulfillment of the requirements for the
Master of Science (Neuroscience)

Department of Cellular and Molecular Medicine
Faculty of Medicine
University of Ottawa

© Susan Ellen Elizabeth MacGowan, Ottawa, Canada, 2026

Abstract

Introduction: Individuals with PTSD can see danger in safe places, and some may feel most alive in high-stress situations. Compared to healthy controls, individuals with PTSD show altered engagement of self-referential processing regions, which may show diminished connectivity during rest and atypical recruitment during threat. Conversely, regions involved in threat prediction, detection, and response show increased connectivity across both threat and resting-state conditions in PTSD. Alpha-desynchronizing electroencephalogram-neurofeedback (EEG-NFB) is a non-invasive brain-training approach that has shown preliminary promise in improving PTSD symptoms.

Methods: Our study tracked individuals with PTSD over 20 weeks of EEG-NFB to evaluate shifts in resting-state functional connectivity (rs-FC) of two key brain regions: the periaqueductal gray (PAG, implicated in threat/defensive responding) and the posterior cingulate cortex (PCC, involved in self-referential processing). At baseline, 36 participants with PTSD were compared to 36 age-matched healthy controls. The PTSD group was randomized in a double-blind fashion to 20 weeks of either experimental EEG-neurofeedback (n = 18; alpha downregulation at Pz) or a sham control (n = 18; yoked sham-signal). Psychological assessments and resting-state functional magnetic resonance imaging (fMRI) scans were conducted at baseline and post-treatment, with an additional clinical assessment at 3-month follow-up. Seed-based rs-FC analyses of the PAG and PCC were performed to evaluate baseline and post-treatment differences (FWE whole-brain corrected, $p < .05$).

Results: At baseline, participants with PTSD, as compared to healthy controls, showed increased PAG rs-FC with the left amygdala (involved in fear and emotional processing), as well as decreased right PCC rs-FC with the bilateral precuneus (part of the default mode network implicated in self-referential functions). The experimental group showed significant pre-to-post NFB changes in rs-FC, significant within-group reductions in PTSD symptom severity (Clinician Administered PTSD Scale [CAPS]), and 61.1% (11/18) no longer met diagnostic criteria, compared with 33.3% (6/18) in the sham-control group. Here, the experimental group showed decreased dorsolateral PAG (dlPAG) rs-FC with the right bed nucleus of the stria terminalis/nucleus accumbens and the bilateral superior colliculus (regions important for reward/threat prediction and detection, respectively). Additionally, the experimental group showed increased rs-FC between PCC regions and the bilateral precentral and middle frontal gyri (implicated in motor planning, executive function, and attention regulation) and between the right PCC and the visual network's left calcarine cortex. Pre-to-post NFB increases in ventrolateral PAG (vlPAG) rs-FC with the left calcarine cortex correlated with greater reductions in the average within-session alpha amplitude percentage change in the experimental group. Additionally, post-NFB increased left PCC rs-FC with the salience network's right mid/anterior insula correlated with lower post-treatment Multiscale Dissociation Inventory (MDI) scores in the experimental group. Finally, greater pre-to-post NFB decreases in dlPAG rs-FC with the default mode network's left PCC correlated with greater reductions in CAPS scores in the experimental group.

Conclusion: These findings provide preliminary evidence that alpha-desynchronizing EEG-NFB may offer a targeted intervention for PTSD. Our results suggest that EEG-NFB may quiet an overactive threat system in PTSD by reducing dlPAG rs-FC with regions involved in threat prediction, detection, and response, while simultaneously restoring self-related connectivity through increased PCC rs-FC with frontal regions.

Acknowledgments

I would like to express my sincere gratitude to my thesis supervisor, Dr. Andrew Nicholson, for the opportunity to conduct this research in his lab. I am very grateful for the experience I gained under your supervision, as well as for the guidance and academic framework you provided, which allowed me to develop this project with purpose.

I extend my sincere thanks to Maria Densmore for creating a warm and supportive learning environment. Your guidance in instructing me on the various methods for running my data analyses was instrumental in developing my skills and confidence to tackle project challenges. I enjoyed our regular meetings and all the laughs we shared together.

I also want to recognize my "NeuroLab twin," Olivia Ardilliez. I appreciate the many hours we spent together in classes, brainstorming secondary research, and sharing the ups and downs of our separate thesis paths. Your camaraderie, humour, and intellectual support made our days in the lab even brighter.

My heartfelt appreciation goes to everyone in the Nicholson NeuroLab, including Brendan, Jill, Lorenzo, Niki, Sandhya, Jon, Ally, Victoria, Emma L, Emma T, Vangel, Matteo, Mengfan, and Ella. I have had the pleasure of knowing and working with you over the past few years. The shared enthusiasm and passion for science made the lab an enriching place to learn and grow. I am especially grateful for the supportive, curious, and intellectually generous environment which shaped my development as a researcher.

I would also like to thank my committee members, Dr. Andra Smith and Dr. Natalia Jawarska, for donating your valuable time, support, and expertise to refine this work. Additionally, I am incredibly grateful to the Neuroscience program director, Dr. Diane Lagace, for answering my many questions, providing administrative support, and encouraging me throughout my graduate studies.

I gratefully acknowledge the financial support that made this work possible, including funding from the National Legion Foundation's Master's Scholarship, the Canada Graduate Scholarship – Master's (Canadian Institutes of Health Research), the University of Ottawa Entrance Scholarship, the Institute of Mental Health Research at the Royal's Genevieve MacKinnon Award, and a stipend from the Atlas Institute for Veterans and Families. Their support gave essential resources that enabled me to pursue this research and complete my graduate studies.

Finally, none of this would have been possible without my family. I want to recognize my partner, Abdel, and my beautiful children—Valencia, Dahlia, Troy, and Rachel. Thank you for your unconditional love, endless patience, and deep understanding while I balanced the demands of intensive research and graduate studies alongside our many family commitments.

Table of Contents

Abstract ... ii
Acknowledgments ... iii
Table of Contents ... v
List of Tables ... vii
List of Figures ... viii
Abbreviations ... ix
1. Introduction ... 1
1.1 PTSD Neurobiology ... 1
1.2 Neurofeedback as a PTSD Treatment ... 5
1.3 Original work ... 8
1.4 Hypotheses ... 8
2. Methods ... 9
2.1 Participants ... 9
2.2 Experimental design ... 11
2.3 EEG recording, preprocessing and analysis ... 12
2.4 EEG-NFB paradigm ... 12
2.5 fMRI paradigm and image acquisition ... 14
2.6 fMRI preprocessing ... 14
2.6.1 fMRI whole-brain preprocessing ... 14
2.6.2 fMRI SUIT space preprocessing ... 15
2.6.3 Seed time-course regressors ... 15
2.7 Connectivity analyses ... 17
2.7.1 First-level connectivity analyses ... 17
2.7.2 Second-level connectivity analyses ... 17
2.7.3 Clinical comparisons at baseline ... 18
2.7.4 Change in clinical measures ... 19
2.7.5 NFB performance ... 19
2.7.6 NFB performance and PTSD severity correlations with rs-FC ... 20
3. Results ... 20
3.1 Baseline demographic and clinical characteristics ... 20
3.2 Baseline rs-FC results ... 20
3.3 NFB performance ... 23
3.4 Changes in PTSD symptoms ... 23
3.5 Pre-to-post NFB rs-FC results ... 25
3.6 NFB performance correlations with rs-FC patterns ... 27
3.7 PTSD symptom severity correlations with rs-FC patterns ... 28
4. Discussion ... 29

4.1 First hypothesis: baseline differences 29
4.2 Second hypothesis: experimental within-group pre- to post-NFB changes 32
4.3 Third hypothesis: correlation with NFB performance 35
4.4 Fourth hypothesis: correlations with clinical scores 36
5. Limitations and future directions 37
6. Conclusion 38
References 40

List of Tables

Table 1. Baseline participant demographic and clinical information

Table 2. Baseline full factorial ANOVAs: 2 (group) x 2 (subregion)

Table 3. Baseline seed-based rs-FC comparisons between participants with PTSD and healthy controls

Table 4. PTSD severity (CAPS) outcome measure

Table 5. Pre-to-post NFB full factorial ANOVAs: 2 (group) x 2 (time) and 2 (group) x 2 (time) x 2 (subregion)

Table 6. Pre-to-post NFB seed-based rs-FC within-group comparisons for the experimental and sham-control groups

Table 7. Seed-based rs-FC multiple regression analyses for the experimental group

List of Figures

Figure 1. Experimental design

Figure 2. Masks for PCC seed-based analyses

Figure 3. Masks for PAG seed-based analyses

Figure 4. Masks for *a priori* ROI analyses

Figure 5. Baseline seed-based rs-FC comparisons between participants with PTSD and healthy controls

Figure 6. Alpha amplitude within-sessions and across-sessions

Figure 7. PTSD severity (CAPS) change

Figure 8. Pre-to-post NFB seed-based rs-FC within-group comparisons for the experimental group

Figure 9. Seed-based rs-FC multiple regression analyses for the experimental group

Abbreviations

AAL	Automated Anatomical Labelling
ACC	Anterior Cingulate Cortex
AC-PC	Anterior Commissure-Posterior Commissure
ANOVA	Analysis of Variance
ART	Artifact Detection Tools
BNST	Bed Nucleus of the Stria Terminalis
BOLD	Blood-Oxygen-Level-Dependent
CAPS	Clinician-Administered PTSD Scale
CEN	Central Executive Network
CTQ	Childhood Trauma Questionnaire
dACC	Dorsal ACC
dlPAG	Dorsolateral PAG
DMN	Default Mode Network
DSM	Diagnostic and Statistical Manual
EEG	Electroencephalogram
EPI	Echo Planar Imaging
Exp	Experimental Group
FFT	Fast Fourier Transform
FOV	Field of View
FWE	Family-Wise Error
FWHM	Full-Width-at-Half-Maximum
fMRI	Functional MRI
Hz	Hertz
IAS	Innate Alarm System
ICA	Independent Component Analysis
IIR	Infinite Impulse Response
LEC-5	Life Events Checklist for DSM-5
lPCC	Left PCC
mPFC	Medial Prefrontal Cortex
MPRAGE	Magnetization-Prepared Rapid Acquisition Gradient Echo
MDD	Major Depressive Disorder
MDI	Multiscale Dissociation Inventory
MNI	Montreal Neurological Institute
MRI	Magnetic Resonance Imaging

NAc	Nucleus Accumbens
NFB	Neurofeedback
ns	Not Significant
PAG	Periaqueductal Gray
PCC	Posterior Cingulate Cortex
PFC	Prefrontal Cortex
PNS	Parasympathetic Nervous System
Pz	Midline Parietal Electrode
RCT	Randomized Controlled Trial
ROI	Region of Interest
rPCC	Right PCC
rs-FC	Resting-State Functional Connectivity
SC	Superior Colliculus
SCID	Structured Clinical Interview for DSM
Sham	Sham-Control Group
SN	Salience Network
SNS	Sympathetic Nervous System
SPL	Superior Parietal Lobule
SPM12	Statistical Parametric Mapping 12
SSRI	Selective Serotonin Reuptake Inhibitor
SNRI	Serotonin-Norepinephrine Reuptake Inhibitor
SUIT	Spatially Unbiased Infratentorial Template
TE	Echo Time
TR	Repetition Time
vlPAG	Ventrolateral PAG

1. Introduction

Post-traumatic stress disorder (PTSD) is a debilitating psychiatric condition that may arise following exposure to one or more traumatic events and is characterized by intrusive memories, avoidance, negative alterations in cognition and mood, and heightened arousal and reactivity (American Psychiatric Association, 2022). Individuals with PTSD frequently demonstrate persistent threat sensitivity even in safe environments and may also display atypical engagement of self-referential brain regions during threat, which may be associated with a stress-related sense of self (Lanius et al., 2020, 2025). Critically, mounting evidence indicates that such alterations in threat processing and self-experience in PTSD are associated with disruptions in neural functional connectivity following trauma (Harricharan et al., 2016; Lanius et al., 2010a; Nicholson et al., 2017, 2020a; Rabellino et al., 2018a, 2018b).

1.1 PTSD Neurobiology

The posterior cingulate cortex (PCC) serves as a core hub within the brain's default mode network (DMN), a large-scale neural network centrally implicated in self-referential cognition, autobiographical memory retrieval, and the ongoing integration of internal and external information (Buckner et al., 2008; Leech & Sharp, 2014). Anatomically, the PCC is densely interconnected with other key DMN nodes, including the medial prefrontal cortex (mPFC), precuneus, and angular gyrus, forming a highly integrated system that supports the construction and maintenance of the self, mental time travel, and contextual appraisal of experience (Andrews-Hanna et al., 2010; Utevsky et al., 2014). Among these regions, the PCC is a functional and structural anchor that coordinates information flow across the DMN (Leech et al., 2011; Whitfield-Gabrieli & Ford, 2012). The coordination is critical for regulating network suppression that facilitates transitions between internal thought and external task engagement (Leech et al., 2011; Whitfield-Gabrieli & Ford, 2012). This renders the PCC particularly vulnerable to network-wide connectivity disruptions, which present as the aberrant resting-state dynamics that are frequently observed in neuropsychiatric conditions, including PTSD (Buckner et al., 2008; Whitfield-Gabrieli & Ford, 2012).

Many resting-state functional magnetic resonance imaging (fMRI) studies demonstrate that PTSD disrupts DMN connectivity, with this dysfunction largely centred in the PCC (Sripada et al., 2012; Whitfield-Gabrieli & Ford, 2012). Indeed, multiple studies report reduced within-DMN connectivity (particularly between the PCC and other DMN nodes such as the mPFC and hippocampus), suggesting a breakdown in the network's integrative function (DiGangi et al., 2016; Koch et al., 2016; Miller et al., 2017; Sripada et al., 2012).

Simultaneously, individuals with PTSD commonly exhibit increased connectivity between the DMN (including the PCC) and salience or threat detection networks, showing a maladaptive coupling that may bias the brain toward persistent threat monitoring at rest (Abdallah et al., 2017; Akiki et al., 2017; DiGangi et al., 2016; Whitfield-Gabrieli & Ford, 2012). Disrupted PCC–mPFC and PCC–hippocampus functional connectivity has been specifically linked to difficulties in autobiographical memory integration, self-referential processing, and contextual appraisal: processes highly relevant to the phenomenology of PTSD (DiGangi et al., 2016; Koch et al., 2016). Moreover, abnormalities in PCC resting-state activity, including both hyperactivity and hypoactivity, have been observed and are thought to underlie core symptoms such as intrusive memories, rumination, dissociative experiences, identity disturbance, and impaired self-soothing (Abdallah et al., 2017; Miller et al., 2017; Whitfield-Gabrieli & Ford, 2012). Collectively, these neuroimaging findings suggest the PCC as a critical node in the biological mechanism of PTSD, which may act as a bridge where self-reflection and trauma-related triggers interact (Akiki et al., 2017; Miller et al., 2017).

Disruptions in PCC and DMN connectivity have direct implications for the clinical presentation of PTSD (Sripada et al., 2012; Whitfield-Gabrieli & Ford, 2012). Aberrant PCC functional coupling is thought to contribute to either persistent self-focus or self-detachment by compromising the DMN's role in self-referential processing (Akiki et al., 2017; Whitfield-Gabrieli & Ford, 2012). When the PCC fails to connect properly with the hippocampus or mPFC, individuals with PTSD struggle to organize autobiographical memories, which may present as fragmented or intrusive trauma recollections and make it difficult to form a coherent life story (DiGangi et al., 2016; Koch et al., 2016). These disruptions also affect "mental time travel"—the ability to envision future scenarios or recall past events—further contributing to identity disturbance and impaired planning observed in PTSD (Abdallah et al., 2017; Miller et al., 2017). Additionally, abnormal PCC activity and connectivity have been linked to dissociative symptoms of depersonalization and derealization, reflecting the DMN's failure to maintain a stable sense of self during rest (Sripada et al., 2012; Whitfield-Gabrieli & Ford, 2012). By interfering with the DMN's capacity to optimally regulate self-experience, altered PCC connectivity thus helps explain several hallmark symptoms of PTSD (Akiki et al., 2017; Miller et al., 2017).

Although the PCC is traditionally conceptualized as a single midline DMN entity, neuroimaging research has started to demonstrate notable functional and connectivity differences between its left and right hemispheres (Saenger et al., 2012; Foster et al., 2023). For example, Saenger et al. (2012) showed that the left PCC (lPCC) has significantly greater

functional connectivity (including to DMN regions), and the right PCC (rPCC) shows contrasting rightward dominance in grey matter volume. Treating the left and right PCC as separate seed regions recognizes their unique structural and functional profiles (Saenger et al., 2012). During traumatic script imagery, Lanius et al. (2005) found that individuals with PTSD showed lower functional connectivity between the lPCC and the rPCC compared to trauma-exposed controls, which may underlie disturbances in self-referential processing and memory recall. However, most resting-state functional connectivity (rs-FC) studies of PTSD use a single midline PCC seed and do not explore hemispheric differences (Bluhm et al., 2009; Lanius et al., 2010a; Qin et al., 2012).

PTSD arousal symptoms—particularly hypervigilance—are increasingly recognized as both a consequence and a driver of altered large-scale network dynamics (Akiki et al., 2017; Menon, 2011). Hyperactivity within the salience network (SN) lowers the threshold for threat detection, leading to the misidentification of benign stimuli as dangerous and perpetuating hyperarousal (Akiki et al., 2017). When the SN is persistently overactive, it can destabilize the resting-state DMN connectivity by disrupting the switching mechanism between the central executive network (CEN) and DMN (Akiki et al., 2017; Menon, 2011). This network dysregulation helps explain how PTSD-related hyperarousal disrupts self-referential processing and contributes to the disorder's core clinical features (Akiki et al., 2017; Menon, 2011).

Notably, aberrant connectivity between the PCC and midbrain structures in PTSD has been implicated in dysfunctional crosstalk between self-referential and threat-processing circuits in the maintenance of PTSD symptoms (Nicholson et al., 2020a; Terpou et al., 2020). Terpou et al. (2020) found that individuals with PTSD, as compared to healthy controls, showed stronger periaqueductal gray (PAG) excitatory effective connectivity to the DMN (precuneus and mPFC) during the subliminal processing of trauma-related cues. Additionally, the strength of this PAG-to-DMN connectivity positively correlated with clinical symptoms of state dissociation and avoidance (Terpou et al., 2020). These findings demonstrate that heightened midbrain threat-detection may disrupt cortical self-referential processing and drive the disconnected or diminished sense of self commonly reported in PTSD (Terpou et al., 2020). Furthermore, Terpou et al. (2019a) introduced the concept of the "threatful-self," which describes how an individual with PTSD's sense of self may be shaped by hypervigilance and anticipatory fear, with experiences of agency and coherence being most accessible in threat-related states (Terpou et al., 2019a). Furthermore, trauma survivors often report a lack of 'feeling alive' unless engaging in high-arousal or sensory-seeking behaviours, which suggests that individuals with PTSD could be drawn to threat-inducing situations to experience a more

embodied self-experience (Lanius et al., 2020, 2025). Indeed, the aftermath of trauma could result in an individual with PTSD's sense of self becoming diminished when at rest and enhanced when under threat (Lanius et al., 2020). These alterations of self-experience in PTSD could be seen as two sides of the same coin; symptoms of threat-anticipating hypervigilance could be inhibiting optimal self-referential processing at rest while also driving a more integrated sense of self in threatening situations (Terpou et al., 2019a; Lanius et al., 2020, 2025).

Threat prediction and detection involve the PAG, a midbrain structure (Corrigan & Christie-Sands, 2020; Lanius et al., 2025) that coordinates subcortical approach or defensive responses (Kearney & Lanius, 2022; Mobbs et al., 2007). The PAG is organized into longitudinal columns, most notably the dorsolateral PAG (dlPAG) implicated in sympathetic nervous system (SNS) active defences of 'fight and flight' and the ventrolateral PAG (vlPAG) implicated in parasympathetic nervous system (PNS) passive defences of 'freeze or immobility' (Benarroch et al., 2012; Harricharan et al., 2016; Terpou et al., 2019b; Vianna et al., 2001; Webb et al., 2020). The defence cascade is a sequence of automatic survival behaviours in response to perceived threat (arousal/on-edge, freeze/scan and detect, fight/flight, tonic immobility, collapsed immobility, and quiescent immobility), where the vlPAG predominates as PNS activation that overrides dlPAG SNS activation when a threat is perceived as inescapable (Harricharan et al., 2016; Kozlowska et al., 2015). Disruptions in PAG functional connectivity in individuals with PTSD are hypothesized to contribute to hyperarousal of the defence cascade (Nicholson et al., 2016a). Harricharan et al. (2016) found that individuals with PTSD, as compared to healthy controls, showed extensive dlPAG and vlPAG rs-FC with areas associated with defensive action and emotional reactivity. Furthermore, distinct roles have been proposed for the dlPAG in mediating active fight-or-flight defensive responses characteristic of classic PTSD, and for the vlPAG in supporting passive coping strategies observed in the dissociative subtype of PTSD (Harricharan et al., 2016).

Additionally, the PAG is a core component of the innate alarm system (IAS), a primarily subcortical network that rapidly detects environmental threats, often before conscious awareness (Lanius et al., 2017; Steuwe et al., 2014; Terpou et al., 2019b). The IAS comprises interconnected nuclei, including the midbrain (superior colliculus [SC], PAG), locus coeruleus, limbic system (amygdala, insula, thalamus) and the right cerebellar lobule V (Terpou et al., 2019b). The SC aids rapid orientation to stimuli and relays this information to the PAG (Corrigan & Christie-Sands, 2020; Lanius et al., 2025). Consequently, subconscious threat detection within the IAS precedes the activation of the defence cascade (Lanius et al., 2017, 2025; Terpou et al., 2019c). Supporting this, individuals with PTSD exhibit IAS overactivation

when exposed to subliminal threat-related stimuli relative to healthy controls (Terpou et al., 2019b). This overactivation suggests that the PAG not only executes defensive reflexes, but functions within active inference models to calculate threat levels and bias the selection of coping strategies (Terpou et al., 2019c; Linson et al., 2020).

Disruptions in PAG connectivity may impair the brain's capacity to generate and update environmental predictions (Lanius et al., 2025; Roy et al., 2014; Solms, 2022). In PTSD, this predictive role may fail if altered PAG connectivity compromises the calculation of mismatch—or prediction error—signals (Lanius et al., 2025; Roy et al., 2014; Solms, 2022). This subcortical breakdown is consistent with clinical evidence showing that individuals with PTSD struggle with basic everyday predictions and over-predict future danger (Eisenberg et al., 2023). When a healthy organism experiences a mismatch between expectations and an actual outcome, its predictive models are typically updated to minimize environmental uncertainty (Arnaldo et al., 2022; Friston, 2010; Friston & Frith, 2015; Friston et al., 2011; Linson et al., 2020). Critically, an individual with PTSD's ability to deploy these adaptive updates may be compromised, resulting in their restricting themselves to highly predictable environments to avoid the uncertainty and surprise associated with prediction errors (Arnaldo et al., 2022; Eisenberg et al., 2023; Lanius et al., 2025; Linson et al., 2020; Solms, 2022).

Although disruptions affect both the DMN and the IAS in PTSD, recent rs-FC studies have begun to specifically disentangle how aberrant coupling between the PAG and PCC may maintain core symptoms (Koch et al., 2016; Nicholson et al., 2020; Terpou et al., 2020). Indeed, as reviewed in this section, altered rs-FC between these regions is hypothesized to reflect a persistent bias toward threat processing at rest, with the PAG's heightened connectivity to cortical midline structures such as the PCC possibly disrupting the self-referential and integrative functions of the DMN (Sripada et al., 2012; Thome et al., 2017). Together, these findings highlight the need for interventions capable of restoring adaptive connectivity among the PAG and PCC to alleviate the persistent network-level disruptions that sustain PTSD symptoms (Koch et al., 2016; Menon, 2011; Nicholson et al., 2020b; Terpou et al., 2020).

1.2 Neurofeedback as a PTSD Treatment

Neurofeedback (NFB) is a non-invasive brain-training technique that enables individuals to self-regulate neural activity by providing real-time feedback, typically through electroencephalogram (EEG) or fMRI signals (Lieberman et al., 2023b; Ros et al., 2014, 2020; Sitaram et al., 2017). During NFB sessions, brain activity is continuously monitored and translated into visual and auditory cues that allow individuals to modify their neural patterns

through practice and reinforcement (Lieberman et al., 2023b; Nicholson et al., 2020b; Ros et al., 2014, 2020; Sitaram et al., 2017). Over time, this process is thought to promote adaptive changes in brain networks underlying various cognitive, emotional and behavioural functions (Lieberman et al., 2023b; Nicholson et al., 2020b; Ros et al., 2020; Sitaram et al., 2017).

Given accumulating evidence that PTSD is characterized by aberrant connectivity between the PAG and PCC (Lanius et al., 2020; Terpou et al., 2020; Webb et al., 2020), interventions capable of directly modulating these neural circuits have become a focus of recent research (Thome et al., 2017; Nicholson et al., 2020b). Evidence shows that both fMRI- and EEG-based approaches can engage circuits central to self-referential and emotional processing regions (Lieberman et al., 2023b; Ros et al., 2014). Supporting the clinical relevance of targeting the PCC, Lieberman et al. (2023b) demonstrated that individuals can learn to self-regulate PCC activity using real-time fMRI NFB. Modulating the PCC versus the amygdala yielded distinct effects on self-referential and emotional processing regions (Lieberman et al., 2023a). Their findings show that PCC-targeted real-time fMRI NFB is especially effective for altering DMN activity and reducing trauma-related symptoms (Lieberman et al., 2023a, 2023b). Additionally, EEG-based NFB studies indicate that this intervention may normalize dysfunctional connectivity patterns among key nodes of the DMN and SN in PTSD (Kluetsch et al., 2014; Nicholson et al., 2020b). Together, these NFB studies suggest that both fMRI- and EEG-based training may facilitate adaptive changes in PCC function and restore DMN integrity in PTSD (Kluetsch et al., 2014; Lieberman et al., 2023a, b; Nicholson et al., 2020b). However, EEG-NFB is more widely available and cost-effective for clinical use than fMRI-NFB (Ros et al., 2020; Sitaram et al., 2017).

Alpha-based EEG-NFB protocols, which focus on enhancing post-training neural oscillatory power in the 8–12 Hz range, have shown potential to normalize DMN connectivity and reduce PTSD symptoms in randomized controlled trials (RCT; Nicholson et al., 2020b). Alpha band oscillations have been closely linked to the functional integrity of the DMN in prior EEG-fMRI research, suggesting that interventions that modulate alpha activity may influence large-scale brain networks implicated in PTSD (Bowman et al., 2017). Notably, alpha rhythms are most evident during relaxed wakefulness and reduced external engagement and are associated with restful states when not engaged in a specific task (Jensen & Mazaheri, 2010; Klimesch, 2012). To clinically target these neural oscillations, EEG-NFB protocols commonly use the Pz (parietal midline) electrode position (Kluetsch et al., 2014; Nicholson et al., 2020b). This site directly overlies major posterior nodes of the DMN; targeting alpha power here modulates broad network dynamics and reduces symptoms in clinical populations (Nicholson

et al., 2020b). Clancy et al. (2020b) found that higher PTSD scores of hypervigilance significantly correlated with reduced alpha-frequency connectivity and alpha-band power within the visual cortex and DMN hubs (PCC and mPFC). Indeed, individuals with PTSD have commonly been observed to have reduced alpha-rhythm at rest, particularly over the DMN's main hubs, and this is hypothesized to be an index of chronic hyperarousal in PTSD (Abdallah et al., 2017; Clancy et al., 2017, 2020b; Liberzon & Abelson, 2016; Nicholson et al., 2020b; Sitaram et al., 2017; Ros et al., 2014).

EEG-NFB training using an alpha-desynchronizing protocol, which reduces within-session alpha amplitude at the Pz electrode, may be an effective treatment for individuals with PTSD (du Bois et al., 2021; Lieberman et al., 2026; Nicholson et al., 2020b, 2023; Shaw et al., 2023). Here, a therapeutic *alpha-rebound effect*, which is a shift of alpha-rhythms towards normalization post-NFB, is thought to occur via mechanisms that regulate the brain's homeostatic excitatory/inhibitory balance (Nicholson et al., 2023; Kluetsch et al., 2014; Sitaram et al., 2017). Indeed, Nicholson et al. (2023) found in a recent RCT that 20 weeks of EEG-NFB alpha-desynchronizing training can rescue reduced alpha-rhythms in individuals with PTSD within mPFC regions of the DMN, providing longitudinal evidence of this alpha-rebound effect of alpha re-synchronization following desynchronizing EEG-NFB. Moreover, Nicholson et al. (2020b) found using independent component analysis (ICA) that individuals with PTSD in the experimental group after treatment displayed decreased PCC connectivity and increased dorsomedial prefrontal cortex (PFC) connectivity with the anterior DMN, as well as decreased precuneus connectivity with the posterior DMN (Nicholson et al., 2020b). The experimental group also demonstrated clinical improvements with significant within-group reductions in PTSD symptom severity (Clinician Administered PTSD Scale [CAPS]) that were maintained at the 3-month follow-up (Nicholson et al., 2020b). Additionally, 61.1% of individuals in the experimental group no longer met the diagnostic criteria for PTSD (CAPS) and were in remission at the end of the trial, as compared to 33.3% in the sham-control group (Nicholson et al., 2020b).

Furthermore, a single 30-minute session of alpha-desynchronizing EEG-NFB was shown in individuals with PTSD to impact PAG rs-FC (Nicholson et al., 2016a) and DMN functional connectivity with the PCC (Kluetsch et al., 2014). Kluetsch et al. (2014) reported a significant alpha-rebound effect at rest following EEG-NFB, linked to increased calmness and enhanced DMN functional connectivity with the bilateral PCC, right middle frontal gyrus, and left mPFC, as measured using ICA. Additionally, Nicholson et al. (2016a) showed pre-NFB left amygdala rs-FC with the PAG using seed-based analyses with a shift in amygdala rs-FC to PFC emotion-

regulation regions after NFB. Here, this increased IAS rs-FC in individuals with PTSD prior to NFB was theorized to reflect heightened defence processing in this population (Nicholson et al., 2016a). Despite these advances, the extent to which multiple sessions of alpha-based EEG-NFB can restore PAG and PCC rs-FC patterns in PTSD remains unknown. As such, the present study aims to address this gap by directly testing whether multi-session EEG-NFB can modulate rs-FC of the PAG (including dlPAG and vlPAG subregions) and PCC (including left and right hemispheres) in individuals with PTSD using a 20-week alpha-desynchronizing protocol.

1.3 Original work

Given that this study uses the same dataset and participants as Nicholson et al. (2020b), the key additions to the original RCT report are seed-based rs-FC analyses of the PAG (with subregions) and PCC (with hemispheric lateralization). Notably, no prior study has examined whether multi-session EEG-NFB can specifically normalize rs-FC among the PAG and PCC—regions implicated in the maintenance of PTSD symptoms (Terpou et al., 2020). By linking these neural changes to symptom reduction, this work provides the first direct evidence for a mechanistic pathway from PAG and PCC remediation to clinical improvement in PTSD, thus advancing both the scientific and translational NFB literature. Additionally, the present study investigates the left and right PCC hemispheres, as well as the dlPAG and vlPAG subregions. Examining hemisphere-specific PCC seeds expands on existing research into the PCC alterations in rs-FC and distinct clinical outcomes (Miller et al., 2017; Viard et al., 2019). Investigating the dlPAG and vlPAG as distinct subregions is warranted, as these subdivisions are implicated in fundamentally different defensive responses, with the dlPAG mediating active fight-or-flight behaviours and the vlPAG subserving passive, dissociative coping strategies (Harricharan et al., 2016; Terpou et al., 2019c). By simultaneously examining rs-FC within lateralized PCC and PAG subregions, this study offers a novel approach to understanding the neural mechanisms underlying PTSD symptom heterogeneity.

1.4 Hypotheses

We investigated changes in rs-FC patterns of the PCC (including left and right hemispheres) and the PAG (including dlPAG and vlPAG subregions) in individuals with PTSD following 20 weeks of EEG-NFB using a randomized, sham-controlled design.

H1a: At baseline, individuals with PTSD will have increased PAG rs-FC to regions involved in threat prediction and detection compared to healthy controls.

H1b: At baseline, individuals with PTSD will have decreased PCC rs-FC to regions involved in self-referential processing compared to healthy controls.

H2a: Following 20 weeks of EEG-NFB, the experimental group will show decreased within-group PAG rs-FC to regions involved in threat detection.

H2b: Following 20 weeks of EEG-NFB, the experimental group will show increased within-group PCC rs-FC to regions involved in self-referential processing.

H3: Greater NFB performance (i. e., greater alpha downregulation during training) will be associated with decreased PAG rs-FC to regions involved in threat detection and increased PCC rs-FC to regions involved in self-referential processing.

H4: Reductions in clinical scores (CAPS and Multiscale Dissociation Inventory [MDI]) following EEG-NFB will be associated with decreased PAG rs-FC to regions involved in threat detection and increased PCC rs-FC to regions involved in self-referential processing.

We anticipate that lPCC and rPCC rs-FC will differ, with the lPCC showing greater connectivity to DMN regions (Saenger et al., 2012). We further expect distinct patterns of rs-FC for the dlPAG and vlPAG that reflect their contrasting defensive behaviours, with the dlPAG showing greater rs-FC to regions involved in active fight-or-flight responses and the vlPAG to those involved in passive dissociative coping strategies (Harricharan et al., 2016; Terpou et al., 2019c).

2. Methods

2.1 Participants

Participants with PTSD were recruited between 2014 and 2018 from the London, Ontario community via advertisements and clinical referrals. The initial neuroimaging sample included 76 participants (n = 36 PTSD; n = 36 healthy controls), but four participants were excluded from the PTSD group due to incomplete baseline resting-state fMRI scans, leaving a final sample of 72 (n = 40 PTSD; n = 36 healthy controls; **Table 1**). The healthy controls completed baseline scans to benchmark aberrant neural network dynamics in PTSD but did not receive an intervention. The 36 adults with PTSD (aged 21–59 years) were randomized to either an experimental EEG-NFB group (n = 18) or a sham-control EEG-NFB group (n = 18); both groups completed pre- and post-intervention fMRI scans (**Figure 1**). Groups did not differ significantly in age or sex, and most participants were female. Furthermore, the prevalence of current major depressive disorder (MDD) and other Axis I diagnoses did not differ significantly between the PTSD groups (experimental group: MDD n = 5, somatization disorder n = 1; sham-control group: MDD n = 7, somatization disorder n = 3, specific phobia n = 1). Four participants per PTSD group met the criteria for the dissociative subtype. Finally, trauma types did not differ

significantly between the experimental group (military trauma: $n = 3$; first responder trauma: $n = 2$; civilian abuse/neglect: $n = 13$) and the sham-control group (military trauma: $n = 3$; first responder trauma: $n = 1$; civilian abuse/neglect: $n = 14$; **Table 1**). The PTSD and healthy control participants in this study were previously reported in Nicholson et al. (2020b).

Table 1

Baseline participant demographic and clinical information

	PTSD Experimental Group	PTSD Sham Control Group	Healthy Control Group
N	18	18	36
Sex	12 females	14 females	23 females
Age	40.28 (12.21)	46.28 (12.37)	40 (10.33)
CAPS-Total	36.86 (10.36)	39.94 (7.83)	0.7 (3.17)*
CTQ	54.61 (19.88)	63.88 (19.94)	33.30 (10.33)*
MDI- Total	52.89 (14.87)	67.88 (20.79)	33.20 (3.34)*
MDD	current = 5, past = 8	current = 7, past = 5	current = 0, past = 0
Somatization Disorder	current = 1, past = 0	current = 3, past = 0	current = 0, past = 0
Specific Phobia	current = 0, past = 0	current = 1, past = 0	current = 0, past = 0
Medication	12	12	0

Note. Baseline participant demographic and clinical information. Brackets indicate standard deviation. For comorbid diagnoses, c= current and p= past diagnoses. Asterisks indicate significantly lower values in the healthy control group. PTSD groups did not differ regarding CAPS, CTQ and MDI scores, as well as MDD and other Axis I disorder diagnoses. Abbreviations: PTSD= post-traumatic stress disorder, CAPS = Clinician Administered PTSD Scale (Normalized to CAPS-5), CTQ = Childhood Trauma Questionnaire (none or minimal childhood trauma = 25-36, moderate = 56-68, extreme trauma > 72), MDI = Multiscale Dissociation Inventory, MDD = Major Depressive Disorder (from Nicholson et al., 2020b).

Participants in the PTSD group were included based on a primary PTSD diagnosis, confirmed using both the CAPS (Blake et al., 1995; Weathers et al., 2013a; version IV: $n = 3$, version 5: $n = 33$) and the Structured Clinical Interview for DSM-IV Axis I Disorders (SCID; First et al., 2002). Both CAPS-IV and CAPS-5 were used as the data collection portion of the study spanned the DSM-IV to DSM-5 transition; earlier participants were assessed with CAPS-IV, and later participants with CAPS-5. Additionally, potentially traumatic events were screened using the self-report Life Events Checklist for DSM-5 (LEC-5; Weathers et al., 2013b).

Exclusion criteria comprised: (1) alcohol or substance use disorder not in sustained full remission within the past three months; (2) lifetime history of bipolar or psychotic disorders; (3) concurrent participation in another trauma-focused psychotherapy; (4) past or current biofeedback treatment; (5) acute suicidality within the past three months; (6) self-injurious behaviours requiring medical attention within the past three months; and (7) unstable living conditions or current involvement in an abusive relationship. Exclusion criteria for the healthy control group consisted of a lifetime Axis I psychiatric disorder (evaluated via the SCID) or PTSD (evaluated via the CAPS), current use of psychotropic medications, or any history of biofeedback training. General exclusion criteria for all participants included standard

contraindications to 3T fMRI screening, pregnancy, significant untreated medical illness, a history of neurological or pervasive developmental disorders, or a previous head injury involving loss of consciousness.

Participants with PTSD receiving psychotropic medications (n = 24) maintained a stable dose prior to the NFB trial. At baseline, the experimental (n = 12) and sham-control (n = 12) groups did not differ significantly by medication status, average class dosage, or medication class. Drug classes included antidepressants (n = 19: 15 SSRIs, 3 SNRIs, 1 tricyclic), sedatives (n = 8: 6 benzodiazepines, 3 cyclopyrrolones), atypical antipsychotics (n = 6), and stimulants (n = 2 methylphenidate). During the trial, five participants increased their dosage: three in the experimental group and two in the sham-control group. Including baseline medication as a separate covariate in subsequent analyses did not change the primary results and introduced only minor variations in cluster size.

This study was approved by the Research Ethics Board at Western University, Canada. Participants provided written, informed consent and received financial compensation. To prevent bias, neither the letter of information nor the consent form disclosed the study hypotheses. Participants with PTSD were informed that they would be randomly assigned to either an experimental or a sham-control neurofeedback group to examine if and how they could learn to regulate their brain activity. After completing the study, participants in the sham-control group were offered active EEG-NFB. For more details on study background and participants, see Nicholson et al. (2020b).

2.2 Experimental design

At baseline, all participants underwent clinical assessments using the CAPS, SCID, MDI, and the Childhood Trauma Questionnaire (CTQ; **Table 1**). Participants diagnosed with PTSD during the assessment were randomly assigned under double-blind conditions to either the experimental or sham-control NFB group (**Figure 1**). Next, participants completed a baseline fMRI session that included a 6-minute eyes-closed resting-state scan. One week later, participants commenced a 20-week course of weekly EEG-NFB sessions. The first session focused on establishing treatment goals, introducing the NFB technology, and collecting baseline EEG recordings. Alpha-rhythm training began during the second session and consisted of 20 minutes of alpha-desynchronizing feedback. Consequently, analyses of neurofeedback training effects focused on alpha dynamics from session 2 onward. One week post-treatment, we conducted a second resting-state fMRI scan and a comprehensive clinical follow-up using the CAPS and SCID. Finally, participants completed a third clinical assessment during a 3-

month follow-up visit (**Figure 1**). The experimental design was previously reported in Nicholson et al. (2020b).

Figure 1

Experimental design

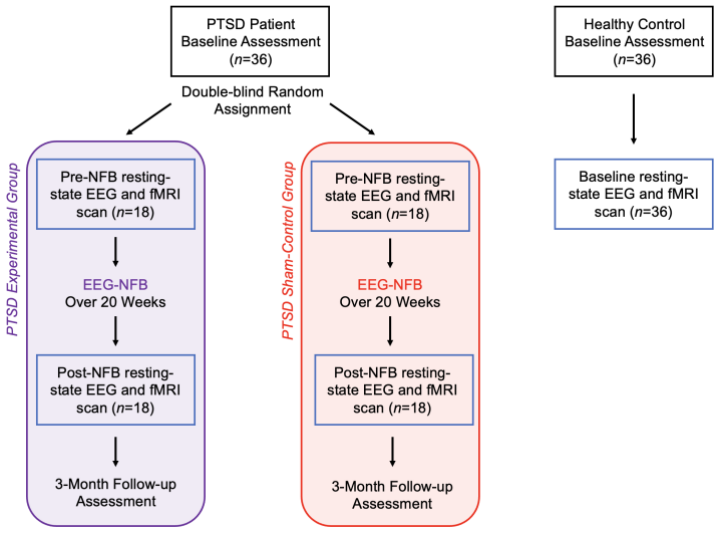

Note. All PTSD participants were compared to healthy controls at baseline using assessments and seed-based rs-FC. PTSD participants were randomly allocated in a double-blind manner to either the active experimental group or sham-control group. Pre-to-post NFB treatment changes in assessments and seed-based rs-FC were compared for the experimental and sham-control groups. Abbreviations: EEG = electroencephalogram, NFB = neurofeedback, PTSD = post-traumatic stress disorder, rs-FC = resting-state functional connectivity, fMRI = functional magnetic resonance imaging (adapted from Nicholson et al., 2020b).

2.3 EEG recording, preprocessing and analysis

Scalp EEG was recorded at 250 Hz using a Phoenix A202 2-channel EEG amplifier. The active, reference, and ground electrodes were placed at Pz (international 10–20 system), the left earlobe (A1), and the right earlobe (A2), respectively. Offline, the raw data were bandpass filtered between 0.5 and 40 Hz and imported into the EEGLAB toolbox within MATLAB. We performed statistical artifact rejection using the FASTER plug-in (Nolan et al., 2010), removing epochs with extremal amplitude or variance deviations exceeding two standard deviations from the mean (|z-score| > 2). Alpha power (8–12 Hz) was estimated via a Fast Fourier Transform (FFT) using Welch's method (Matlab "pwelch" function) with a 2 s Hanning window and 50% overlap. The EEG recording, preprocessing and analysis were previously reported in Nicholson et al. (2020b).

2.4 EEG-NFB paradigm

During the initial NFB session, participants with PTSD established treatment goals, received psychoeducation, and underwent an orientation to the NFB technology while completing a baseline EEG recording. Participants commenced active alpha-desynchronizing EEG-NFB training during the second session. Each subsequent training session began with a

3-minute, open-eyes baseline EEG recording without feedback, during which participants relaxed, gazed at a blank wall, and minimized physical movement.

NFB training was delivered through an interactive game in which visual progression depended on alpha-amplitude suppression. Participants completed 20-minute training sessions divided into six 3-minute blocks and one 2-minute block with performance scores displayed at the end of each block. All participants received identical auditory feedback (single beeps). To accommodate personal preferences and avoid potential emotional triggers, participants chose between two visual feedback modalities: (1) a cartoon moving across the screen, or (2) a grid-divided photograph where individual pieces revealed themselves sequentially.

The experimental group down-regulated alpha amplitude (8–12 Hz) using a real-time EEG feedback signal derived from the midline parietal cortex (Pz electrode), selected because the alpha rhythm is typically maximal there (Ergenoglu et al., 2004). Participants received no explicit regulation strategies and were instructed to explore individual mental techniques.

Sham-control participants followed identical instructions and environmental setups as the experimental participants but received a yoked sham NFB signal replayed from a successful experimental participant to ensure comparable motivational states (Sorger et al., 2019). To maintain the double-blind design, the EEGer sham-training software incorporated real-time artifacts (e.g., eye blinks, muscle movements) into the replayed signal. Following study completion, sham-control participants were offered active EEG-NFB treatment.

We used infinite impulse response (IIR) band-pass filtering to extract alpha oscillations from EEG signals using 0.5-second epochs. The initial reward threshold was set to deliver positive feedback approximately 65% of the time. To maintain this reward density across participants, thresholds were adjusted at the start of each training block based on the preceding 30 seconds of EEG data if the reward rate fell outside the 50–90% window.

Participants completed 17 or more of the 20 available weekly sessions. The mean number of completed sessions was 19.6 (SD = 0.98) for the experimental group and 19.9 (SD = 0.24) for the sham-control group. The mean treatment duration did not differ statistically between groups, with 161.1 days (SD = 36.3) in the experimental group and 182.2 days (SD = 39.7) in the sham-control group. The EEG-NFB paradigm was previously reported in Nicholson et al. (2020b).

2.5 fMRI paradigm and image acquisition

Participants with PTSD completed a 6-minute resting-state fMRI scan before and after the EEG-NFB intervention during separate laboratory visits. Age-matched healthy controls completed only the baseline resting-state fMRI scan, as they did not receive the NFB intervention. For the resting-state paradigm, participants were instructed to close their eyes and avoid focusing on anything in particular while letting their minds wander (Bluhm et al., 2009; Fransson, 2005).

Brain imaging was performed using a 3 T magnetic resonance imaging (MRI) scanner (Trio, Siemens Medical Solutions, Erlangen, Germany) equipped with a 32-channel phased-array head coil. For the resting-state scan, 120 volumes of whole-brain blood-oxygen-level-dependent (BOLD) images were acquired using the manufacturer's standard T2*-weighted gradient-echo planar imaging (EPI) pulse sequence. This sequence utilized single-shot, blipped-EPI, interleaved slice acquisition, and three-dimensional prospective acquisition correction.

The acquisition parameters were as follows: repetition time (TR) = 3000 ms, echo time (TE) = 20 ms, flip angle = 90°, field of view (FOV) = 192 × 192 × 128 mm^3 (matrix size = 94 × 94, 64 slices), and an isotropic voxel resolution of 2 mm. High-resolution T1-weighted anatomical images were also acquired using a Magnetization-Prepared Rapid Acquisition Gradient Echo (MPRAGE) sequence (192 slices, 1 mm isotropic resolution). The fMRI paradigm and image acquisition parameters were previously reported in Nicholson et al. (2020b).

2.6 fMRI preprocessing

2.6.1 fMRI whole-brain preprocessing

Functional image preprocessing was performed using SPM12 (Statistical Parametric Mapping; Wellcome Department of Cognitive Neurology, London, UK) implemented in MATLAB R2024b (MathWorks, Natick, MA). The preprocessing pipeline consisted of the following steps that were previously reported in Nicholson et al. (2020b):

- Artifact Removal & Alignment: Discarding the first 4 volumes to allow for T1 equilibration, reorientation to the anterior commissure-posterior commissure (AC-PC) axis, and spatial alignment to the mean image using a rigid-body transformation.

- Coregistration & Segmentation: Reslicing and coregistration of the functional mean image to the participant's T1 anatomical image. Co-registered images were segmented using the "New Segment" method in SPM12.

- Normalization & Smoothing: Functional images were normalized to the Montreal Neurological Institute (MNI) space and spatially smoothed with a 6-mm full-width-at-half-maximum (FWHM) Gaussian kernel.

- Motion & Filtering: Motion artifacts were addressed using the Artifact Detection Tools (ART) software package (Gabrieli Lab, McGovern Institute for Brain Research, Cambridge, MA) to compute regressors for outlier volumes. Finally, smoothed functional images were bandpass filtered (0.012–0.1 Hz) using software by co-author Jean Théberge.

2.6.2 fMRI SUIT space preprocessing

In preparation for the PAG analysis, we performed additional preprocessing steps using the spatially unbiased infratentorial template (SUIT) toolbox functions in SPM12 to improve normalization of the midbrain, cerebellum, and lower brainstem (Diedrichsen, 2006; Diedrichsen et al., 2009; Terpou et al., 2019a, 2019b). Whole-brain images that had previously been co-registered, AC-PC axis reoriented and realigned were isolated into SUIT space. Next, we normalized and resliced the images in SUIT space and smoothed them with a 4 mm FWHM Gaussian kernel (Terpou et al., 2019a). We also applied bandpass filtering (high-pass 0.012 Hz, low-pass 0.1 Hz) to the SUIT space images, using software developed by co-author Jean Théberge. We used the SUIT space images to create PAG seed time-course regressors.

2.6.3 Seed time-course regressors

We generated our six masks using PickAtlas software (WFU PickAtlas, version 3.0.5; Maldjian et al., 2003; http://fmri.wfubmc.edu/software/pickatlas; RRID: SCR_007378). Mean-centred seed-based time-course regressors were then created by extracting the mean signal intensity time-course for each mask using custom software authored by Jean Théberge (Bluhm et al., 2009; Harricharan et al., 2016). A PCC region of interest (ROI) mask, consisting of a 6 mm radius sphere centred at MNI coordinates x, y, z = 0, -56, 20 (Bluhm et al., 2009; King et al., 2016; **Figure 2**), was used to extract the seed-based time-course for the PCC from the whole-brain preprocessed resting-state images. We repeated the same steps for the left and right PCC ROI masks by selecting either left or right in PickAtlas using the same 6 mm radius sphere centred at MNI coordinates x, y, z = 0, -56, 20 (Bluhm et al., 2009; King et al., 2016; **Figure 2**). A PAG ROI mask, consisting of a 6 mm radius sphere centred at MNI coordinates x, y, z = 0, -32, -11 (**Figure 3**), was applied to 4 mm FWHM smoothed SUIT space images to extract the PAG seed-based time-course regressor (Terpou et al., 2019a, 2019b). For the two PAG subdivision masks, we generated rectangular shapes at the dlPAG (MNI x, y, z = 0, -32, -8.5, extension 6x2x1.5 mm) and the vlPAG (MNI x, y, z = 0, -27, -8, extension 3x1x1 mm) and

applied them to the 4 mm FWHM smoothed SUIT space images to extract the seed-based time-course regressors of the PAG subregions (Harricharan et al., 2016; Ezra et al., 2015; **Figure 3**). Our group previously used these coordinates in rs-FC studies in PTSD (PAG in Terpou et al. 2019a, 2019b; dlPAG and vlPAG in Harricharan et al., 2016; PCC in Bluhm et al., 2009).

Figure 2

Masks for PCC seed-based analyses

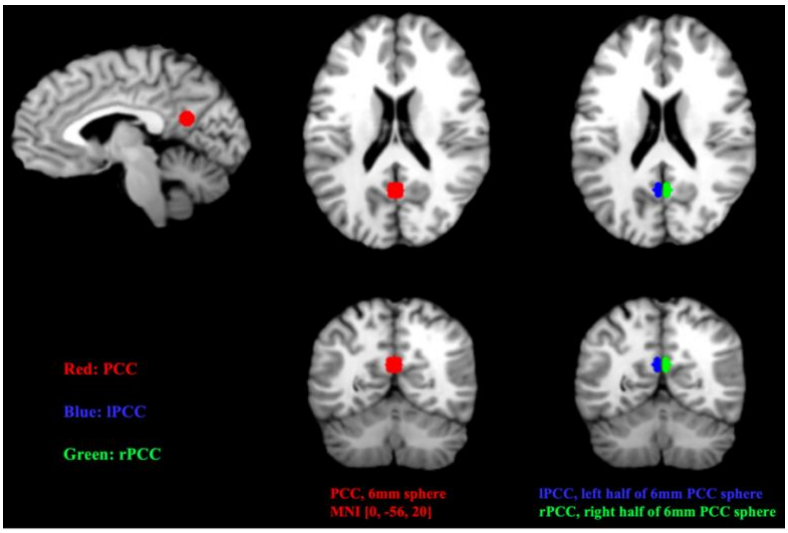

Note. PCC ROIs for seed-based rs-FC analyses using fMRI scans. Abbreviations: ROIs = Regions of Interest, rs-FC = resting-state functional connectivity, fMRI = functional magnetic resonance imaging, MNI = Montreal Neurological Institute, PCC = posterior cingulate cortex, lPCC = left PCC, rPCC = right PCC.

Figure 3

Masks for PAG seed-based analyses

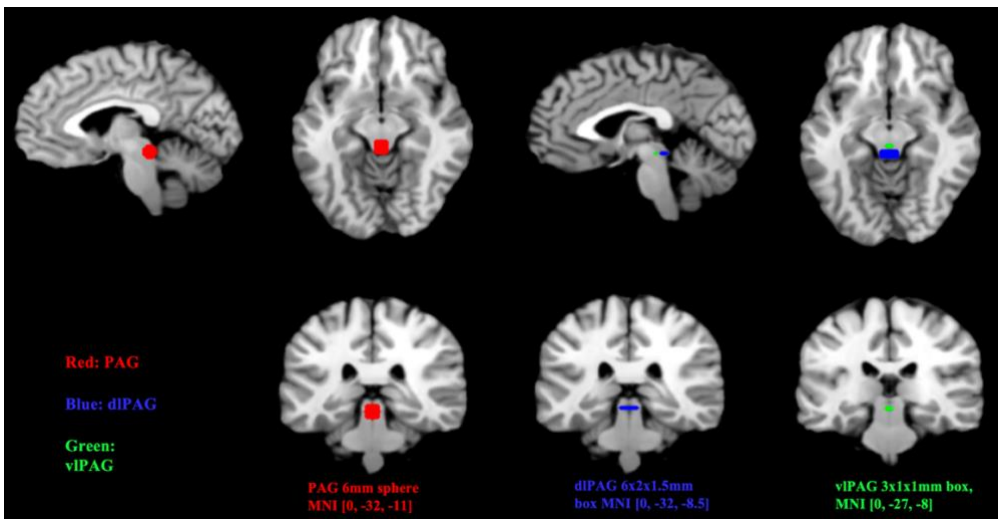

Note. PAG ROIs for seed-based rs-FC analyses using fMRI scans. Abbreviations: ROIs = Regions of Interest, rs-FC = resting-state functional connectivity, fMRI = functional magnetic resonance imaging, MNI = Montreal Neurological Institute, PAG = periaqueductal gray, dlPAG = dorsolateral PAG, vlPAG = ventrolateral PAG.

2.7 Connectivity analyses

2.7.1 First-level connectivity analyses

We completed within-subject first-level analyses for each extracted seed using the 120 whole-brain preprocessed resting-state volumes for each scan (baseline and post-NFB, separately), the ART regressors, and the extracted seed-based time-course regressors (Bluhm et al., 2009; Harricharan et al., 2016). We captured positive correlations between each seed and other voxels in the brain for use in second-level within- and between-group analyses (Bluhm et al., 2009; Harricharan et al., 2016).

2.7.2 Second-level connectivity analyses

For the PCC and PAG seed regions, we examined baseline rs-FC between-group comparisons using separate two-sample t-tests (PTSD vs. healthy control groups). For the lPCC/rPCC and dlPAG/vlPAG baseline analyses, separate 2 (PTSD vs. healthy control groups) x 2 (lPCC and rPCC or dlPAG and vlPAG) full-factorial analyses of variance (ANOVAs) were conducted. Additionally, we conducted separate 2 (experimental and sham-control groups) x 2 (pre- and post-NFB scans) full-factorial ANOVAs to examine changes in both PCC and PAG rs-FC patterns as a function of NFB (Nicholson et al., 2020b). For the dlPAG/vlPAG and lPCC/rPCC analyses, we completed separate 2 (experimental and sham-control group) x 2 (pre- and post-NFB scans) x 2 (dlPAG and vlPAG or lPCC and rPCC) full-factorial ANOVAs to examine changes in PAG and PCC subregion rs-FC as a function of NFB. We completed *a priori* planned within- and between-group t-tests to test our specific hypotheses. In SPM12, an initial voxel-wise thresholding was defined at p-uncorrected $< .001$ $k = 10$, followed by a conservative family-wise error thresholding of p-FWE $< .05$ $k = 10$ to correct for multiple comparisons.

Figure 4

Masks for a priori ROI analyses

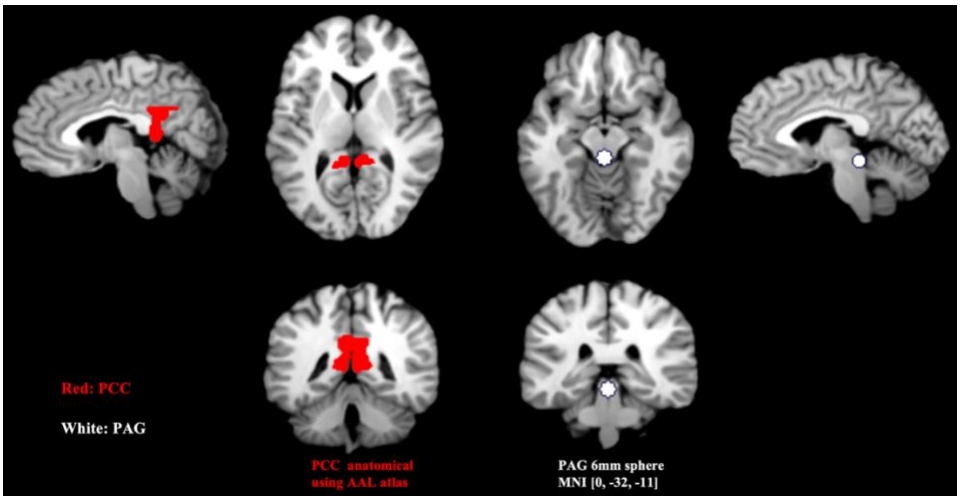

Note. Masks used for small volume correction *a priori* ROI analyses examining the PAG and PCC for the PCC and PAG seed-based rs-FC analyses, respectively, using fMRI scans. Abbreviations: ROIs = regions of interest, rs-FC = resting-state functional connectivity, fMRI = functional magnetic resonance imaging, AAL = automated anatomical labelling, MNI = Montreal Neurological Institute, PCC = posterior cingulate cortex, PAG = periaqueductal gray.

In addition to our whole-brain analyses, we conducted *a priori* ROI analyses examining the PAG with the PCC seed-based analysis and the PCC with the PAG seed-based analysis. Prior research justifies this selection, demonstrating altered functional connectivity between the PAG, PCC, and DMN in PTSD populations (Terpou et al., 2019a; Webb et al., 2020). Our approach builds on the empirical findings from Terpou et al. (2019a), which demonstrated that the PAG subcortical threat-detection circuit significantly altered DMN coupling in PTSD. Conducting seed-based rs-FC analyses using these *a priori* ROIs allowed us to detect alterations between these two regions by examining the connectivity between the PAG's bottom-up midbrain survival signalling and the PCC's top-down self-referential architecture (Terpou et al., 2020) at baseline and following EEG-NFB. For our analysis, we generated a single anatomical mask of the PCC using PickAtlas according to the Automated Anatomical Labelling (AAL) atlas and inspected it to ensure proper PCC identification (Harricharan et al., 2016; **Figure 4**). In PickAtlas, we generated a single PAG mask consisting of a 6 mm radius sphere that was centred at MNI coordinates x, y, z = 0, -32, -11 (Terpou et al., 2019a, 2019b; **Figure 4**). We used the same p-FWE < .05, k = 10 statistical thresholds as in our whole-brain analysis.

2.7.3 Clinical comparisons at baseline

Nicholson et al. (2020b) previously evaluated and reported on baseline clinical comparisons between both the PTSD experimental and sham-control groups as well as the healthy control and PTSD groups. In that prior work, independent-samples t-tests were used to compare baseline values between groups for participant age and clinical measures on the CAPS,

CTQ, and MDI. Additionally, Pearson's chi-squared and Fisher's exact tests were used to compare between-group differences in current major depressive disorder diagnoses, other Axis I disorder diagnoses, and sex. As these baseline comparisons have already been thoroughly examined and published, these statistical tests were not repeated for the present study.

2.7.4 Change in clinical measures

Nicholson et al. (2020b) previously evaluated and reported on changes in PTSD symptom severity using CAPS scores as the primary outcome measure (**Table 4**; **Figure 7**). During data collection, an updated CAPS-5 was released, and all responses were normalized to the CAPS-5 scale by dividing participants' CAPS-IV scores (3 participants in total) by the maximum CAPS-IV score and then multiplying by the maximum CAPS-5 score. In that prior work, SPSS (version 26) was used to conduct behavioural statistical analyses, including a split-plot repeated-measures ANOVA to evaluate changes on the CAPS with the within-subject factor of time (pre-NFB, post-NFB, 3-month follow-up) and the between-subjects factor of group (PTSD experimental and sham-control groups). For examining CAPS within-group changes, paired-samples t-tests were performed. Independent-samples t-tests were performed to compare CAPS scores between the PTSD experimental and sham-control groups at post-NFB and 3-month follow-up. Nicholson et al. (2020b) used a Bonferroni correction for multiple comparisons in post hoc tests evaluating changes in CAPS ($p = 0.05/6$). As these analyses on PTSD symptom severity have already been thoroughly examined and published, these statistical tests were not repeated for the present study.

2.7.5 NFB performance

Nicholson et al. (2020b) previously evaluated and reported on NFB performance (**Figure 6**). For the alpha-desynchronizing protocol, successful EEG-NFB performance was defined by a reduction in alpha amplitude within each session. Specifically, performance was quantified as the percent change in alpha amplitude during the training periods relative to the initial baseline rest period. Each 20-minute NFB session consisted of seven training periods (six 3-minute periods and one 2-minute period), and the average alpha amplitude across these periods was compared to the session's baseline to calculate the percent reduction (**Figure 6A**). A greater reduction in alpha amplitude over the course of a session reflected superior performance, consistent with the goals of the alpha-desynchronizing protocol. As NFB performance metrics and analyses have already been thoroughly reported, these evaluations were not repeated in the present study.

2.7.6 NFB performance and PTSD severity correlations with rs-FC

Multiple regression analyses evaluated the associations between rs-FC patterns—specifically within the PCC (including lPCC and rPCC) and PAG (including dlPAG and vlPAG)—and both clinical scores and EEG-NFB average alpha amplitude percentage change. We examined these relationships at baseline (pre-NFB), post-intervention (post-NFB), and across time (pre-to-post changes). The techniques for multiple regression analyses were previously reported in Nicholson et al. (2020b).

For the baseline analysis, we regressed pre-NFB rs-FC maps against pre-NFB clinical symptom scores. To assess longitudinal changes, rs-FC difference maps (both pre-minus-post and post-minus-pre NFB z-scores) were calculated for each participant using the SPM12 ImCalc function. These difference maps served as the dependent variable in linear regression models, with independent variables consisting of average alpha amplitude percentage change and clinical symptom change scores (pre-minus-post and post-minus-pre NFB CAPS and MDI scores, respectively). The post-NFB models included post-NFB rs-FC maps as the dependent variable, predicted by the same change scores alongside absolute post-NFB clinical symptom scores.

3. Results

3.1 Baseline demographic and clinical characteristics

At baseline, participants with PTSD, as compared to age-matched healthy controls, had significantly higher total scores for PTSD symptom severity (CAPS), childhood trauma exposure (CTQ), and trauma-related dissociation (MDI; **Table 1**). We found no significant differences at baseline between the PTSD experimental and sham-control groups with respect to age, sex, current comorbid psychiatric conditions (somatization disorder, MDD, and specific phobias), total scores for PTSD symptom severity (CAPS), childhood trauma exposure (CTQ), and trauma-related dissociation (MDI; **Table 1**). Baseline data and statistical comparisons of demographic and clinical characteristics were previously reported in Nicholson et al. (2020b), and we did not repeat these tests in the present study.

3.2 Baseline rs-FC results

At baseline before NFB treatment, we found a significant main effect of group for the lPCC/rPCC ANOVA and a significant main effect of subregion for the dlPAG/vlPAG ANOVA (**Table 2**). More specifically, we found a significant main effect of group for the lPCC/rPCC with the left superior parietal lobule (SPL) and bilateral precuneus (**Table 2**). We also found a

significant main effect of subregion for the dlPAG/vlPAG with the bilateral PAG, bilateral pons and bilateral thalamus (**Table 2**). All other main effects and interactions for the ANOVAs were non-significant.

We found between-group differences in PCC and PAG rs-FC patterns in participants with PTSD as compared to healthy controls at baseline (**Table 3**; **Figure 5**). Here, participants with PTSD, as compared to healthy controls, had decreased PCC rs-FC with the left fusiform gyrus, as well as decreased lPCC rs-FC with the left inferior occipital gyrus (**Table 3**; **Figure 5**). The participants with PTSD, as compared to healthy controls, also had decreased rPCC rs-FC with the bilateral precuneus and the left SPL (**Table 3**; **Figure 5**). By contrast, participants with PTSD, as compared to healthy controls, had increased PAG rs-FC with the left amygdala. Baseline rs-FC group comparisons for the dlPAG and vlPAG were non-significant at this conservative threshold (**Table 3**; **Figure 5**). Additionally, for all ROIs, seed-based rs-FC patterns at baseline did not differ significantly between the PTSD experimental and sham-control groups.

Table 2

Baseline full factorial ANOVAs: 2 (group) x 2 (subregion)

Seed ROIs	Main Effect	Brain Region	Cluster Size	MNI Coordinate			*F* stat.	*Z* score	Peak *p*FWE
				x	y	z			
lPCC/rPCC	Group	Left Superior Parietal Lobule	2274	-20	-76	48	28.21	4.93	0.025
		Bilateral Precuneus	Subpeak	-2	-46	62	27.57	4.87	0.032
		Bilateral Precuneus	Subpeak	0	-56	62	27.09	4.83	0.039
dlPAG/vlPAG	Subregion	Bilateral PAG	1901	-4	-34	-10	228.32	Inf	< 0.001
		Bilateral Pons	Subpeak	2	-34	-18	41.08	5.87	< 0.001
		Bilateral Thalamus	Subpeak	-2	-2	6	38.96	5.73	< 0.001

Note. Baseline seed-based rs-FC full factorial ANOVAs pre-NFB treatment among participants with PTSD (*n* = 36) and healthy controls (*n* = 36). All other main effects and interactions were non-significant (voxel-wise pFWE < 0.05, k = 10). Abbreviations: NFB = neurofeedback, PTSD = post-traumatic stress disorder, ROIs = regions of interest, rs-FC = resting-state functional connectivity, MNI = Montreal Neurological Institute, FWE = family-wise error, ANOVA = analyses of variance, FWE = family-wise error, PCC = posterior cingulate cortex, lPCC = left PCC, rPCC = right PCC, PAG = periaqueductal gray, dlPAG = dorsolateral PAG, vlPAG = ventrolateral PAG.

Table 3

Baseline seed-based rs-FC comparisons between participants with PTSD and healthy controls

Seed ROI	Contrast	Brain Region	Cluster Size	MNI Coordinate			t stat.	Z score	Peak *p*FWE
				x	y	z			
PCC	All PTSD > Healthy Control	*ns*							
	Healthy Control > All PTSD	Left Fusiform Gyrus	22	-38	-38	-22	5.18	4.75	0.045
	PTSD Exp > PTSD Sham	*ns*							
	PTSD Sham > PTSD Exp	*ns*							

lPCC	All PTSD > Healthy Control	*ns*							
	Healthy Control > All PTSD	Left Inferior Occipital Gyrus	318	-44	-70	-18	4.99	4.78	0.044
	PTSD Exp > PTSD Sham	*ns*							
	PTSD Sham > PTSD Exp	*ns*							
rPCC	All PTSD > Healthy Control	*ns*							
	Healthy Control > All PTSD	Bilateral Precuneus	4521	-2	-46	62	5.46	5.19	0.007
		Bilateral Precuneus	Subpeak	0	-56	62	5.42	5.15	0.008
		Left Superior Parietal Lobule	Subpeak	-20	-76	48	5.38	5.12	0.010
	PTSD Exp > PTSD Sham	*ns*							
	PTSD Sham > PTSD Exp	*ns*							
PAG	All PTSD > Healthy Control	Left Amygdala	75	-30	2	-20	5.30	4.84	0.037
	Healthy Control > All PTSD	*ns*							
	PTSD Exp > PTSD Sham	*ns*							
	PTSD Sham > PTSD Exp	*ns*							
dlPAG	All PTSD > Healthy Control	*ns*							
	Healthy Control > All PTSD	*ns*							
	PTSD Exp > PTSD Sham	*ns*							
	PTSD Sham > PTSD Exp	*ns*							
vlPAG	All PTSD > Healthy Control	*ns*							
	Healthy Control > All PTSD	*ns*							
	PTSD Exp > PTSD Sham	*ns*							
	PTSD Sham > PTSD Exp	*ns*							

Note. Baseline seed-based rs-FC comparisons pre-NFB treatment among participants with PTSD (n = 36) and healthy controls (n = 36; voxel-wise pFWE < 0.05, k = 10). All participants with PTSD were grouped at baseline for comparison with age-matched healthy controls. Additionally, we report that the baseline seed-based rs-FC analyses did not differ significantly between the PTSD experimental (n = 18) and sham-control (n = 18) groups. Abbreviations: NFB = neurofeedback, PTSD = post-traumatic stress disorder, ROI = region of interest, rs-FC = resting-state functional connectivity, MNI = Montreal Neurological Institute, FWE = family-wise error, Healthy Control = healthy-control group, Exp = experimental group, Sham = sham-control group, *ns* = not significant, PCC = posterior cingulate cortex, lPCC = left PCC, rPCC = right PCC, PAG = periaqueductal gray, dlPAG = dorsolateral PAG, vlPAG = ventrolateral PAG.

Figure 5

Baseline seed-based rs-FC comparisons between participants with PTSD and healthy controls

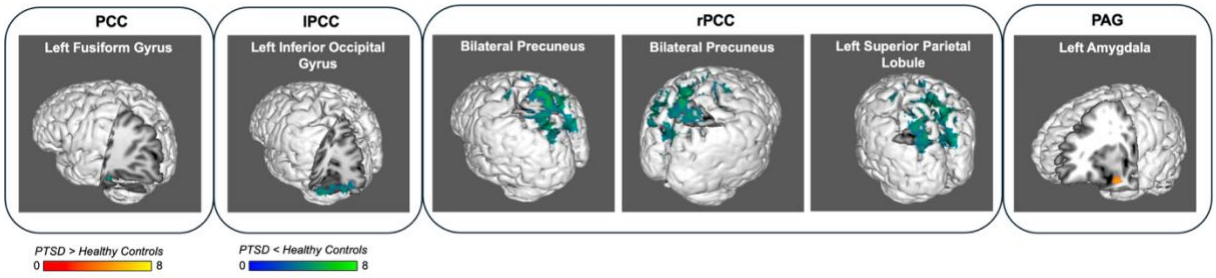

Note. Baseline seed-based rs-FC comparisons pre-NFB treatment between PTSD participants (n = 36) and healthy controls (n = 36) using PCC and PAG ROIs and their subregions (voxel-wise pFWE < .05, k = 10). Abbreviations: NFB = neurofeedback, PTSD = post-traumatic stress disorder, ROIs = regions of interest, rs-FC = resting-state functional connectivity, FWE = family-wise error, PCC = posterior cingulate cortex, lPCC = left PCC, rPCC = right PCC, PAG = periaqueductal gray.

3.3 NFB performance

Results on NFB training performance in this study have been previously reported (see Nicholson et al., 2020, 2023 for details), and these tests were not repeated in the present study. In summary, however, the experimental group showed a more sustained reduction in alpha amplitude during NFB training sessions compared to the sham-control group (**Figure 6A**). Longitudinal mapping across all training sessions further demonstrated that the experimental group consistently maintained greater reductions in alpha amplitude compared to rest than the sham-control group throughout the intervention period (**Figure 6B**).

Regarding subjective regulation strategies, most participants reported attempting to "quiet their mind." Other reported strategies included focusing on the colours of the NFB interface, imagining oneself inside the displayed photo, or mentally focusing on the auditory reward beeps triggered by alpha suppression. Additionally, no participants in either the experimental or sham-control group dropped out of the study, indicating EEG-NFB tolerability.

Figure 6

Alpha amplitude within-sessions and across-sessions

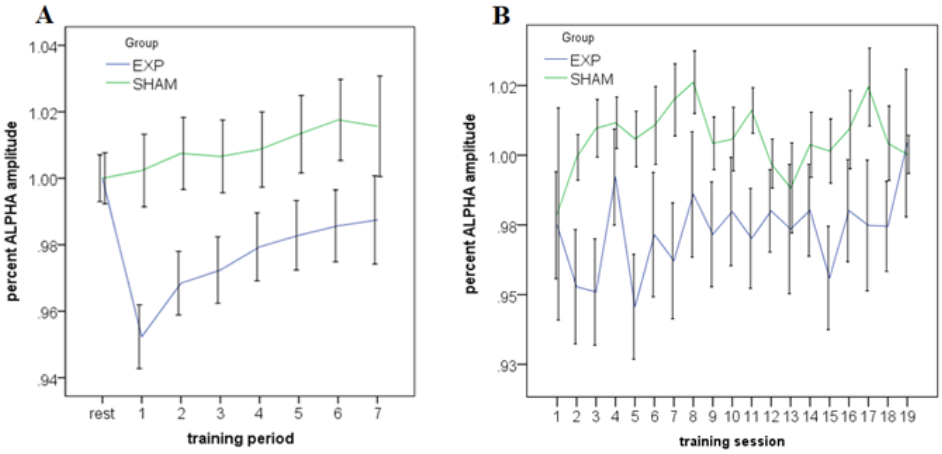

Note. A. Within-session alpha amplitude for the experimental NFB group and the sham-control NFB group averaged over all NFB-training sessions (1-19). Rest represents the initial 3-min rest period recorded directly before training, and the subsequent feedback training was subdivided into 7 periods (over 20 min total). Alpha amplitude at the feedback site (channel Pz) was expressed as percentage change relative to the rest baseline of the respective session. B. Across-session alpha amplitude for the experimental NFB group and the sham-control NFB groups averaged over all training periods (1-7). Alpha amplitude was expressed as percent change relative to the rest baseline of the respective session. Error bars represent ± 1 SEM. Abbreviations: NFB = neurofeedback, Exp = experimental group, Sham = sham-control group, Pz = parietal midline electrode position, SEM = standard error of the mean (from Nicholson et al., 2020b).

3.4 Changes in PTSD symptoms

Results pertaining to improvements in PTSD symptom severity have been previously reported elsewhere (see Nicholson et al., 2020, 2023 for details), and these tests were not repeated for the present study. In brief, participants in the PTSD experimental group demonstrated significant reductions in CAPS-total scores from pre- to post-NFB and at the 3-

month follow-up, whereas the sham-control group did not show significant change across these time points (**Table 4**; **Figure 7**). In the experimental group, 61.1% (11/18) no longer met diagnostic criteria for PTSD, compared with 33.3% (6/18) in the sham-control group. Every participant in remission achieved a clinically meaningful reduction >30% in their CAPS scores (Halvorsen, 2016). Compared to baseline, only the experimental group showed clinically meaningful mean score reductions at post-NFB (33.8%) and at the 3-month follow-up (36.0%). Reductions within the sham-control group remained below the threshold of clinical significance at both post-NFB (17.9%) and the 3-month mark (20.4%) (**Table 4**; **Figure 7**). No significant differences in symptom severity were observed between the experimental and sham-control groups at either the post-NFB or 3-month follow-up assessments.

Table 4

PTSD severity (CAPS) primary outcome measure

	PTSD Experimental Group			PTSD Sham-Control Group		
	Pre-NFB	Post-NFB	3- Month Follow-up	Pre-NFB	Post-NFB	3-Month Follow-up
CAPS-Total	36.86 (10.36)	24.39 (15.61)*	23.58 (14.09) *	39.94 (7.83)	32.78 (12.27)	31.78 (12.86)
% CAPS Reduction	-	33.8% (Clinically meaningful reduction)	36.0% (Clinically meaningful reduction)	-	17.9%	20.4%
Result Summary	-	Reduced compared to Pre-NFB (p < .008, dz = 0.71)	Reduced compared to Pre-NFB (p < .005, dz = 0.77)	-	*ns* (dz = 0.56)	*ns* (dz = 0.63).

Note. The primary outcome measure of PTSD severity (CAPS) at pre-NFB baseline, post-NFB and 3-month follow-up in the experimental and sham-control groups. Abbreviations: NFB = neurofeedback, PTSD= post-traumatic stress disorder, CAPS = Clinician-Administered PTSD Scale (normalized to CAPS-5), *ns* = not significant. *Indicates significantly reduced clinical measures within a PTSD group as compared to pre-NFB baseline.

Figure 7

PTSD severity (CAPS) change

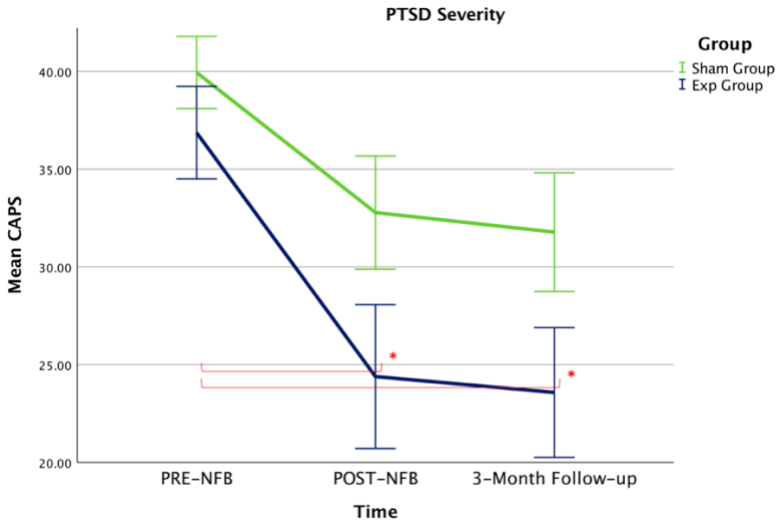

Note. The primary outcome measure of PTSD severity (CAPS) changed significantly over the NFB-intervention for the experimental NFB group as compared to baseline measures. No significant changes were detected in the sham-control group during the NFB intervention compared with baseline measures. Error bars represent standard deviation across participants. Abbreviations: NFB = neurofeedback, PTSD = post-traumatic stress disorder, Exp =

experimental group, Sham = sham-control group, CAPS = Clinician-Administered PTSD Scale (normalized to CAPS-5; from Nicholson et al., 2020b).

3.5 Pre-to-post NFB rs-FC results

Pre-to-post NFB, we found a significant main effect of time for the PCC, lPCC/rPCC and dlPAG/vlPAG ANOVAs and a significant main effect of subregion for the dlPAG/vlPAG ANOVA (**Table 5**). More specifically, we found a significant main effect of time for the PCC with the right precentral gyrus (**Table 5**). Additionally, we found a significant main effect of time for the lPCC/rPCC with the right precentral gyrus, right middle/superior frontal gyri, left middle frontal gyrus, left precentral gyrus, and bilateral anterior cingulate cortex (ACC; **Table 5**). We also found a significant main effect of time for the dlPAG/vlPAG with the bilateral PAG (**Table 5**). Finally, we found a significant main effect of subregion for the dlPAG/vlPAG with the bilateral pons and bilateral hypothalamus (**Table 5**). All other main effects and interactions for the ANOVAs were non-significant.

Direct planned comparisons revealed significant within-group changes in PCC, lPCC, rPCC and dlPAG rs-FC patterns over the course of NFB treatment for participants in the experimental group (**Table 6**; **Figure 8**). Specifically, the experimental group showed increased PCC rs-FC with the right precentral/middle frontal gyri post-NFB as compared to pre-NFB (**Table 6**; **Figure 8**). There were also increased lPCC rs-FC with the left precentral gyrus, the right precentral/middle frontal gyri, and the left middle frontal/precentral gyri post-NFB as compared to pre-NFB in the experimental group (**Table 6**; **Figure 8**). The experimental group showed, post-NFB compared with pre-NFB, increased rPCC rs-FC with the right precentral/middle frontal gyri, bilateral medial superior frontal gyri, the right superior frontal gyrus, the left middle frontal gyrus, and the left calcarine cortex (**Table 6**; **Figure 8**). For the dlPAG seed, we found that post-NFB, as compared with pre-NFB, the experimental group showed decreased dlPAG rs-FC with the right bed nucleus of the stria terminalis (BNST)/nucleus accumbens (NAc) and the bilateral SC (**Table 6**; **Figure 8**). For the other PAG seeds, we did not observe significant experimental within-group differences in the rs-FC analyses (**Table 6**). Notably, we did not detect significant within-group differences in rs-FC in the sham-control group for any seed (**Table 6**). We also did not find significant between-group differences pre- or post-NFB when comparing the experimental and sham-control groups.

Table 5

Pre-to-post NFB full factorial ANOVAs: 2 (group) x 2 (time) and 2 (group) x 2 (time) x 2 (subregion)

Seed ROIs	Main Effect	Brain Region	Cluster Size	MNI Coordinate			*F* stat.	*Z* score	Peak *p*FWE
				x	y	z			
PCC	Time	Right Precentral Gyrus	388	36	-6	58	30.50	4.87	0.030
lPCC/ rPCC	Time	Right Precentral Gyrus	2804	36	-6	58	41.00	5.86	< 0.001
		Right Middle/ Superior Frontal Gyri	Subpeak	30	4	62	36.46	5.55	< 0.001
		Left Middle Frontal Gyrus	Subpeak	-30	2	52	27.80	4.89	0.026
		Left Precentral Gyrus	158	-32	-18	62	32.65	5.27	< 0.001
		Bilateral Anterior Cingulate Gyrus	33	2	26	-4	28.80	4.97	0.018
dlPAG/vlPAG	Time	Bilateral PAG	303	8	-30	-8	29.05	4.99	0.018
	Subregion	Bilateral Pons	217	-2	-36	-4	72.06	7.52	< 0.001
		Bilateral Hypothalamus	77	4	-6	-12	27.63	4.88	< 0.001

Note. Pre-to-post NFB treatment seed-based rs-FC full factorial ANOVAs among participants with PTSD in the experimental (*n* = 18) and sham-control (*n* = 18) groups. All other main effects and interactions were non-significant (voxel-wise *p*FWE < 0.05, *k* = 10). Abbreviations: NFB = neurofeedback, PTSD = post-traumatic stress disorder, ROIs = regions of interest, rs-FC = resting-state functional connectivity, MNI = Montreal Neurological Institute, FWE = family-wise error, ANOVA = analyses of variance, PCC = posterior cingulate cortex, lPCC = left PCC, rPCC = right PCC, PAG = periaqueductal gray, dlPAG = dorsolateral PAG, vlPAG = ventrolateral PAG.

Table 6

Pre-to-post NFB seed-based rs-FC within-group comparisons for the experimental and sham-control groups

Seed ROI	Group	Contrast	Brain Region	Cluster Size	MNI Coordinate			t stat.	Z score	Peak *p*FWE
					x	y	z			
PCC	Exp.	Pre > Post NFB	*ns*							
		Post > Pre NFB	Right Precentral/ Middle Frontal Gyri	372	38	-4	58	5.59	5.05	0.012
	Sham	Pre > Post NFB	*ns*							
		Post > Pre NFB	*ns*							
lPCC	Exp.	Pre > Post NFB	*ns*							
		Post > Pre NFB	Left Precentral Gyrus	3239	-32	-18	62	5.75	5.43	0.002
			Right Precentral/ Middle Frontal Gyri	Subpeak	38	-4	58	5.69	5.38	0.002
			Left Middle Frontal Gyrus	Subpeak	-32	2	50	5.54	5.25	0.005
	Sham	Pre > Post NFB	*ns*							
		Post > Pre NFB	*ns*							
rPCC	Exp.	Pre > Post NFB	*ns*							
		Post > Pre NFB	Right Precentral/ Middle Frontal Gyri	1523	36	-6	58	6.01	5.65	0.001
			Bilateral Medial Superior Frontal Gyrus	Subpeak	0	26	64	5.50	5.21	0.005
			Right Superior Frontal Gyrus	Subpeak	20	0	58	5.28	5.03	0.013
			Left Middle Frontal Gyrus	486	-32	2	50	5.48	5.20	0.006
			Left Calcarine Cortex	82	-6	-66	10	5.15	4.91	0.022
	Sham	Pre > Post NFB	*ns*							
		Post > Pre NFB	*ns*							

PAG	Exp.	Pre > Post NFB	*ns*							
		Post > Pre NFB	*ns*							
	Sham	Pre > Post NFB	*ns*							
		Post > Pre NFB	*ns*							
dlPAG	Exp.	Pre > Post NFB	Bilateral Superior Colliculus	277	8	-32	-6	5.54	5.25	0.005
			Right Bed Nucleus of the Stria Terminalis/ Nucleus Accumbens	60	6	2	6	4.99	4.77	0.042
		Post > Pre NFB	*ns*							
	Sham	Pre > Post NFB	*ns*							
		Post > Pre NFB	*ns*							
vlPAG	Exp.	Pre > Post NFB	*ns*							
		Post > Pre NFB	*ns*							
	Sham	Pre > Post NFB	*ns*							
		Post > Pre NFB	*ns*							

Note. Pre-to-post NFB treatment seed-based rs-FC comparisons for the PTSD experimental (n = 18) and sham-control (n = 18) groups (voxel-wise pFWE < 0.05, k = 10). Abbreviations: NFB = neurofeedback, PTSD = posttraumatic stress disorder, ROI = region of interest, rs-FC = resting-state functional connectivity, MNI = Montreal Neurological Institute, FWE = family-wise error, Exp. = experimental group, Sham = sham-control group, *ns* = not significant, PCC = posterior cingulate cortex, lPCC = left PCC, rPCC = right PCC, PAG = periaqueductal gray, dlPAG = dorsolateral PAG, vlPAG = ventrolateral PAG.

Figure 8

Pre-to-post NFB seed-based rs-FC within-group comparisons for the experimental group

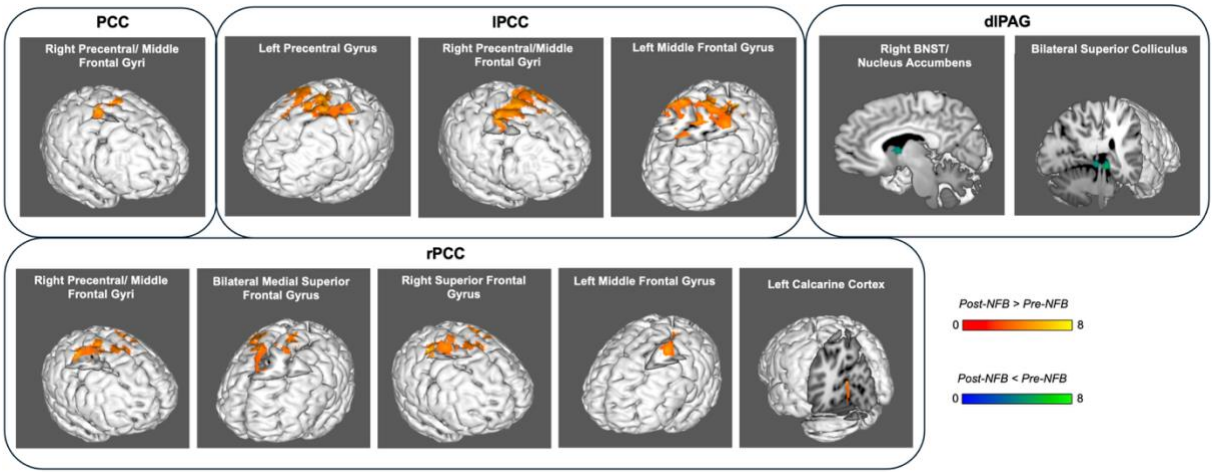

Note. Pre-to-post NFB treatment seed-based rs-FC within-group comparison results unique to the PTSD experimental group (n = 18; voxel-wise pFWE < .05, k = 10). Abbreviations: NFB = neurofeedback, PTSD = post-traumatic stress disorder, ROIs = regions of interest, rs-FC = resting-state functional connectivity, FWE = family-wise error, PCC = posterior cingulate cortex, lPCC = left PCC, rPCC = right PCC, PAG = periaqueductal gray, dlPAG = dorsolateral PAG, BNST = bed nucleus of the stria terminalis.

3.6 NFB performance correlations with rs-FC patterns

We found a significant correlation with NFB performance for the experimental group using the vlPAG seed region. Using the post-NFB minus pre-NFB vlPAG difference maps, a negative correlation was found between the alpha amplitude percent change (**Figure 6A**) and vlPAG rs-FC with the left calcarine cortex (**Table 7**; **Figure 9**). This showed that greater reductions in alpha amplitude within-session were associated with increased rs-FC between the

vlPAG and left calcarine cortex. For the other seeds, we did not observe significant rs-FC results in the multiple regression analyses.

3.7 PTSD symptom severity correlations with rs-FC patterns

We found significant correlations with PTSD symptom severity change for the experimental group using the dlPAG and lPCC seed regions. For the *a priori* PCC ROI analysis, we found a positive correlation between CAPS 1-2 clinical scores (pre-minus-post NFB CAPS scores; **Table 4**) and dlPAG rs-FC with the left PCC using the pre-minus-post NFB dlPAG difference maps (**Table 7**; **Figure 9**). In other words, greater reductions in PTSD symptom severity following NFB were associated with decreased rs-FC between the dlPAG and left PCC. Using post-NFB lPCC rs-FC scans, a negative correlation was found between post-NFB MDI scores and lPCC rs-FC with the right mid/anterior insula (**Table 7**; **Figure 9**). For the other seeds and clinical scores, we did not observe significant rs-FC results in the multiple regression analyses.

Table 7

Seed-based rs-FC multiple regression analyses for the experimental group

Seed ROI	Group	Contrast	Brain Region	Cluster Size	MNI Coordinate			t stat.	Z score	Peak *p*FWE
					x	y	z			
lPCC	Exp.	MDI Post-NFB, Neg. Correlation	Right Mid/ Anterior Insula	86	36	2	10	7.91	4.98	0.043
dlPAG*	Exp.	CAPS 1-2, Post < Pre-NFB, Pos. Correlation	Left Posterior Cingulate Cortex	26	-8	-50	20	5.32	3.98	0.019
vlPAG	Exp.	Alpha %, Post > Pre-NFB, Neg. Correlation	Left Calcarine Cortex	42	-16	-72	10	7.98	5.00	0.037

Note. Seed-based rs-FC multiple regression analyses for pre-minus-post, post-minus-pre, and post-NFB correlations for the PTSD experimental group. All other multiple regression analyses were non-significant (n = 18; voxel-wise pFWE < 0.05, k = 10). Abbreviations: NFB = neurofeedback, PTSD = post-traumatic stress disorder, ROI = region of interest, rs-FC = resting-state functional connectivity, MNI = Montreal Neurological Institute, FWE = family-wise error, Exp. = experimental group, lPCC = left posterior cingulate cortex, PAG = periaqueductal gray, vlPAG = ventrolateral PAG, MDI = Multiscale dissociation inventory, CAPS = Clinician-administered PTSD scale (normalized to CAPS-5), Alpha % = average alpha amplitude percent change relative to the rest baseline of each respective session, * *a priori* PCC ROI small volume correction.

Figure 9

Seed-based rs-FC multiple regression analyses for the experimental group

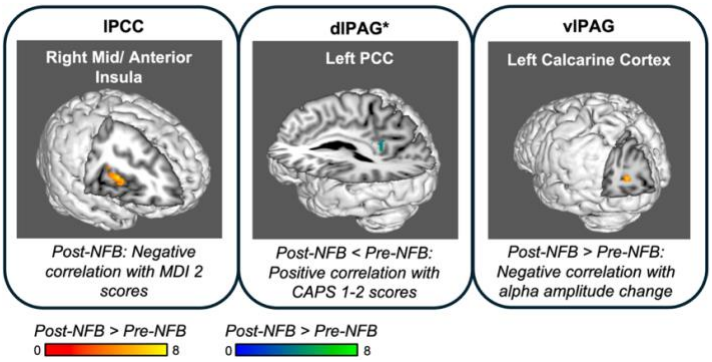

Note. Seed-based multiple regression analyses for pre-minus-post, post-minus-pre, and post-NFB correlations for the PTSD experimental group (n = 18; voxel-wise pFWE < .05, k = 10). Abbreviations: NFB = neurofeedback, PTSD = post-traumatic stress disorder, ROIs = regions of interest, rs-FC = resting-state functional connectivity, FWE = family-wise error, PCC = posterior cingulate cortex, lPCC = left PCC, PAG = periaqueductal gray, dlPAG = dorsolateral PAG, vlPAG = ventrolateral PAG, MDI 2 scores = multiscale dissociation inventory scores post-NFB, CAPS = clinician administered PTSD scale, alpha amplitude change = average alpha amplitude percent change relative to the rest baseline of each respective session, * = *a priori* PCC ROI small volume correction.

4. Discussion

This study demonstrates that 20 weeks of alpha-desynchronizing EEG-NFB may modulate rs-FC among key midbrain and cortical regions implicated in PTSD. Specifically, we observed that participants who received active NFB treatment showed alterations in rs-FC among the PAG and the PCC—regions central to threat detection and self-referential processing, respectively. These neurobiological changes were accompanied by substantial clinical improvements, with a higher proportion of the experimental group no longer meeting diagnostic criteria for PTSD post-treatment compared to the sham-control group.

To contextualize these findings, we will first discuss baseline group differences among individuals with PTSD as compared to healthy controls, highlighting alterations in PAG and PCC rs-FC that were observed prior to the NFB intervention. Next, we review the effects of EEG-NFB on rs-FC in the experimental group, focusing on changes in connectivity within the defensive, self-referential, and executive control networks. We will then examine the relationship between NFB performance and rs-FC changes, and finally, we will explore how these neural alterations relate to clinical symptom improvements and dissociative outcomes. This structured approach allows for a detailed consideration of each hypothesis and its implications for understanding and treating PTSD.

4.1 First hypothesis: baseline differences

At baseline, participants with PTSD exhibited distinct aberrations in rs-FC patterns compared to healthy controls, supporting our first hypothesis and replicating prior results

(Nicholson et al., 2016a). Specifically, participants with PTSD, compared to healthy controls, showed increased rs-FC between the PAG and amygdala—two core regions of the IAS involved in rapid, often subconscious, threat detection and emotional processing (**Table 3**; **Figure 5**; Kozlowska et al., 2015; Lanius et al., 2017). The amygdala is critical for emotion processing and fear responses (Adolphs et al., 2002) as well as threat prediction (Enten et al., 2025). Interestingly, this is a larger-scale replication of Nicholson and colleagues' (2016a) baseline result before completing a single session of alpha-based NFB. In that study, amygdala connectivity following NFB had shifted away from the PAG and towards the mPFC, an area important in emotion regulation (Nicholson et al., 2016a). This subcortical hyperconnectivity likely contributes to the hyperarousal and defensive responses characteristic of PTSD and echoes findings that EEG-NFB can shift amygdala connectivity toward prefrontal regulatory circuits (Nicholson et al., 2016a).

In parallel, we observed decreased rs-FC in participants with PTSD compared to healthy controls between the rPCC and both the bilateral precuneus and left SPL—regions integral to DMN functioning, spatial awareness, and multisensory self-processing (**Table 3**; **Figure 5**; Blanke et al., 2015; Cavanna & Trimble, 2006; Tanaka & Kirino, 2021). The precuneus is crucial for episodic memory and self-referential thought (Cavanna & Trimble, 2006; Utevsky et al., 2014), while the SPL underpins spatial orientation and multisensory integration (Blanke et al., 2015). Hypoconnectivity within these regions has been linked to disturbances in bodily self-consciousness, narrative identity, and multisensory processing in PTSD (Koch et al., 2016; Rabellino et al., 2018b). Such decoupling within the posterior DMN in our clinical cohort underscores a fundamental breakdown within the posterior DMN midline, consistent with recent models of trauma-induced network dysregulation (Azarias et al., 2025). Mechanistically, such hypoconnectivity may underlie the altered sense of self and fragmented autobiographical memory often reported by trauma survivors (Lanius et al., 2020; Spreng & Grady, 2009; Yehuda et al., 2015). Thus, our findings of disrupted DMN connectivity may parallel the narrative fragmentation and identity disturbances that are hallmark features of PTSD (Lanius et al., 2010b; Brewin, 2011; Sutin & Robins, 2007; Yehuda et al., 2015).

Further, we observed decreased PCC rs-FC with the left fusiform gyrus alongside decreased lPCC rs-FC with the left inferior occipital gyrus in participants with PTSD compared to healthy controls (**Table 3**; **Figure 5**). Both the fusiform and inferior occipital gyri are critical processing hubs embedded within the ventral visual stream and the broader visual network (Wang et al., 2017). Typically, functional coupling between the PCC and these visual regions supports visual mental imagery and the vivid retrieval of autobiographical memories (Pearson

et al., 2015; Spreng & Grady, 2009), cognitive processes that are characteristically altered or dysregulated in trauma-exposed populations (Bluhm et al., 2009; Lanius et al., 2010a). Notably, this disrupted DMN–visual network connectivity can be interpreted within the predictive coding framework, in which impaired top-down modulation from self-referential hubs like the PCC may lead to heightened sensory prediction errors and increased uncertainty (Friston, 2010; Linson et al., 2020). In this model, reduced modulation from DMN regions such as the PCC may leave sensory areas (including the fusiform and occipital gyri) more susceptible to unfiltered or overwhelming visual input, consistent with the sensory disinhibition literature in PTSD (Northoff & Bermpohl, 2004; Clancy et al., 2020a, 2020b; Blanke et al., 2015; Rabellino et al., 2018b). The fusiform gyrus, crucial for social and emotional perception, may thus fail to integrate contextual predictions, reducing the ability to accurately interpret safety cues in the environment (Kanwisher et al., 1997; Peelen & Downing, 2005; Adolphs, 2009; Friston, 2010). This impaired gating not only contributes to hypervigilance, intrusive imagery, and difficulties distinguishing relevant from irrelevant sensory information, but also undermines the synthesis of sensory information necessary for coherent self-representation and memory—an interpretation further supported by multisensory integration frameworks (Blanke et al., 2015; Rabellino et al., 2018b). Such impairments may, in turn, manifest behaviorally as fragmented autobiographical recall and hypervigilant visual scanning, hallmark features of PTSD (Bluhm et al., 2009; Lanius et al., 2010a; Brewin, 2014).

Taken together, these baseline findings delineate a model of PTSD, in which subcortical hyperconnectivity within threat-detection circuitry (e.g., PAG–amygdala) perpetuates a state of heightened vigilance and defensive responding, while hypoconnectivity within the DMN and its connections to parietal and visual networks (e.g., PCC–precuneus/SPL, PCC–fusiform/occipital gyri) undermines the integration of sensory information and the coherence of self-related processing (Azarias et al., 2025; Cavanna & Trimble, 2006; Terpou et al., 2019b). This pattern of network dysregulation provides a mechanistic foundation for core clinical features of PTSD, including persistent hyperarousal, fragmented autobiographical memory, and a disrupted sense of self, even in the absence of external threat (Brewin, 2011; Lanius et al., 2010b; Yehuda et al., 2015). Although our results are limited to resting-state parameters, they reveal a foundational alteration in neural organization that may underlie both the chronicity and complexity of PTSD's symptomatology (Koch et al., 2016; Whitfield-Gabrieli & Ford, 2012; Akiki et al., 2017; Lanius et al., 2010b) and is in line with the extant literature (Bao et al., 2021; Koch et al., 2016; Ross & Cisler, 2020; Xiao et al., 2022).

4.2 Second hypothesis: experimental within-group pre- to post-NFB changes

Pre-to-post NFB, the results supported our second hypothesis. Indeed, the experimental group post-NFB, compared to pre-NFB, showed a decrease in dlPAG rs-FC with a cluster encompassing the right BNST and the right NAc (**Table 6**; **Figure 8**). The BNST is a subcortical structure that is involved in threat anticipation and sustained reactivity (Rabellino et al., 2018a). In contrast, the NAc is central to reward/motivational processing and is relevant to stress-induced reward-seeking behaviour in PTSD (Lokshina et al., 2021). Within the framework of active inference and predictive processing (Friston et al., 2015; Roy et al., 2014), this altered connectivity provides compelling neurobiological evidence of updated internal models of threat. In PTSD, the brain operates under rigid, maladaptive top-down "priors"—overestimating environmental danger and maintaining a perpetual state of high-precision threat anticipation (Somerville et al., 2010; Rabellino et al., 2018a). As a key subcortical hub for sustained reactivity to unpredictable cues, the BNST typically amplifies these threat predictions (Brinkmann et al., 2017; Siminski et al., 2021), while concurrent hypoactivation of the NAc blunts prediction errors related to safe or rewarding outcomes, driving anhedonia and emotional numbing (Lokshina et al., 2021). Critically, the dlPAG serves as a primary downstream effector for deploying active defensive responses (Harricharan et al., 2016). The reduced rs-FC observed between the dlPAG and this BNST-striatal network following alpha-desynchronizing EEG-NFB may suggest a normalization of this inflexible predictive loop.

Additionally, the experimental group displayed a decrease in dlPAG rs-FC with the IAS's bilateral SC (**Table 6**; **Figure 8**; Terpou et al., 2019a). Structurally and functionally, the SC and PAG form a critical midbrain circuit thought to mediate the initial, pre-cognitive orienting response of the defence cascade, priming autonomic and motor pathways for survival prior to cortical awareness (Corrigan & Christie-Sands, 2020; Terpou et al., 2019c; Lanius et al., 2017). Indeed, neuroimaging evidence confirms that individuals with PTSD exhibit distinct, pathological alterations in SC resting-state networks at baseline, underscoring a chronic state of subconscious threat processing (Olivé et al., 2018). Within a predictive processing framework, the SC acts as a major subcortical collector of sensory prediction errors, rapidly computing visual and auditory salience to update top-down spatial priors (Parr & Friston, 2017; de Lange et al., 2018). In PTSD, this midbrain loop exhibits pathological hyperconnectivity and assigns excessive importance to low-level sensory inputs, causing the brain to misinterpret harmless environmental stimuli as highly reliable signals of impending threat (Kearney & Lanius, 2024; Putica & Agathos, 2024). Consequently, individuals with PTSD may fail to downgrade these trauma-based threat predictions or assimilate bottom-up safety cues during

neutral resting-state conditions (Kearney & Lanius, 2024; Putica & Agathos, 2024). The post-NFB attenuation of dlPAG-SC functional connectivity observed here suggests that alpha-desynchronizing EEG-NFB may reduce the strength of connectivity within this subcortical sensory pathway. By decreasing the strength of these low-level threat-related signals, NFB potentially "quiets" the automated, hyperarousal-driven orienting responses, thereby enabling a shift toward more flexible, cortically mediated appraisal mechanisms. Taken together, these novel results may collectively suggest a downregulation of the dlPAG's role in both heightened threat anticipation (via the BNST-striatal network; Walker et al., 2003) and reacting to overly sensitive subcortical warning signals (via the SC).

Interestingly, although we observed significant experimental within-group pre-to-post NFB differences in dlPAG rs-FC patterns, we did not observe significant experimental within-group changes in the vlPAG (**Table 6**). The absence of significant vlPAG changes is a meaningful null result as it suggests the intervention selectively quieted active fight/flight defences (dlPAG) without significantly altering passive immobility defences (vlPAG) in our sample (Bandler et al., 2000; Kozlowska et al., 2015). Only a small minority of our PTSD cohort (4 out of 18 participants; 22%) exhibited the dissociative subtype, a distribution that closely mirrors the typical prevalence rates (15–30%) documented in broader clinical trauma populations (Wolf et al., 2012a, b). The dlPAG orchestrates active fight/flight defences and hyperarousal characteristic of non-dissociative PTSD, whereas the vlPAG mediates passive immobility, emotional detachment, and depersonalization/derealization symptoms characteristic of the dissociative subtype (Harricharan et al., 2016; Lanius et al., 2010a). Within an active inference framework, the non-dissociative PTSD phenotype operates under threat predictions that continuously prime active defensive strategies (Kearney & Lanius, 2024). Conversely, the distinct, rigid interoceptive priors that gate passive shut-down mechanisms (Kearney & Lanius, 2024) via descending prefrontal-PAG pathways characteristic of the dissociative subtype (Harricharan et al., 2016; Nicholson et al., 2017) would not be expected to feature prominently in a sample dominated by hyperarousal.

Furthermore, consistent with our second hypothesis, the experimental group demonstrated increased rs-FC between PCC seeds and frontal regions from pre- to post-NFB. When examining the lPCC and rPCC separately, we found increased post-NFB rs-FC with large bilateral clusters spanning the precentral, middle frontal, and superior frontal gyri in the experimental group (**Table 6**; **Figure 8**). When using the full PCC 6mm sphere, we found a smaller right cluster that also spanned the precentral and middle frontal gyri (**Table 6**; **Figure 8**). This heightened coupling with the precentral, middle frontal, and superior frontal gyri is

particularly noteworthy, as these regions act as critical hubs for motor planning, executive function, and top-down attention regulation, respectively (Miller et al., 2001; Stuss, 2011). Additionally, the lPCC connectivity encompasses a larger cluster than the rPCC, which may align with prior work indicating stronger lPCC functional connectivity than rPCC (Saenger et al., 2012). In PTSD, the DMN-mediated sense of self is fragmented and decoupled from regulatory prefrontal executive networks (Lanius et al., 2020). Our result of increased connectivity between the PCC and these specific frontal nodes parallels the findings of Kluetsch et al. (2014), who showed that a single 30-minute NFB session was associated with a significant *alpha rebound effect*, increased calmness, and enhanced DMN functional connectivity involving the bilateral PCC, right middle frontal gyrus, and left mPFC. Beyond supporting our initial hypothesis, these results may indicate a mechanism by which EEG-NFB facilitates top-down regulation of arousal and self-referential processing in PTSD, potentially contributing to clinical symptom reduction (Menon, 2011; Akiki et al., 2017). The pattern of increased PCC–frontal connectivity could reflect a normalization of network dynamics toward those observed in healthy controls (Miller et al., 2017), underscoring NFB's neuroplastic potential. Ultimately, these results could point towards a clinically relevant restoration of DMN rs-FC in participants with PTSD following EEG-NFB treatment, driven by renewed integration with frontal executive networks (Akiki et al., 2017; Miller et al., 2017; Ros et al., 2014).

Additionally, the experimental group also displayed an increase in rPCC rs-FC pre-to-post NFB with the visual network's left calcarine cortex (**Table 6**; **Figure 8**). The calcarine cortex is a primary hub for visual processing (Meadows, 2011; Wandell et al., 2007) and exhibits altered baseline connectivity and sensory-gating deficits in trauma-exposed populations (Harnett et al., 2025). In healthy states, alpha-band oscillations act as an inhibitory computational filter, enabling high-level DMN nodes to modulate the "precision" or gain assigned to low-level visual prediction errors (Clancy et al., 2020b). In PTSD, however, chronic alpha dysrhythmia drives sensory disinhibition, leading to hyper-precise, ungated visual inputs that disrupt the DMN's self-processing loops (Clancy et al., 2020b). Clinically, this manifests as an inability to suppress visual reminders of trauma, resulting in intrusive flashbacks and hypervigilance (Brewin, 2014; Clancy et al., 2020a; Lanius et al., 2010a). Consequently, this novel post-NFB increase in rPCC–calcarine connectivity may reflect not only restored top-down modulation and improved sensory gating, but also a broader reorganization of large-scale network dynamics—a phenomenon widely recognized as a hallmark of adaptive change following psychiatric intervention (Fox & Greicius, 2010; Menon, 2011). Such network reorganization likely indicates a shift toward more normative or efficient DMN–visual network

configurations, which may support accurate contextualization of visual prediction errors and potentially reduce trauma-related visual intrusions (Clancy et al., 2020a; Scheinost et al., 2013).

Taken together, these concurrent pre-to-post NFB alterations provide compelling, multi-network evidence for a potential shift in functional connectivity for individuals with PTSD following active treatment (Lanius et al., 2020; Nicholson et al., 2020a). By simultaneously down-regulating subcortical survival loops—specifically the dlPAG-SC and dlPAG-BNST/striatum pathways—and up-regulating DMN integration via PCC-PFC, alpha-desynchronizing EEG-NFB appears to remediate the profound imbalance between survival-driven active defensive posturing and resting-state homeostasis (Kearney & Lanius, 2024; Putica & Agathos, 2024). Far from merely altering isolated functional pathways, this dual mechanism suggests that NFB facilitates a fundamental transition from an inflexible, defence-oriented brain state to a more adaptive, self-referential configuration capable of genuine rest (Azarias et al., 2025; Kluetsch et al., 2014; Lanius et al., 2020). Consequently, these findings expand our understanding of EEG-NFB as a non-invasive intervention (Nicholson et al., 2016a).

4.3 Third hypothesis: correlation with NFB performance

Our third hypothesis—that NFB performance and changes in rs-FC are associated—was partially supported. Specifically, NFB performance—characterized by a larger magnitude decrease within-session alpha amplitude percentage change—correlated with post-minus-pre NFB increased vlPAG rs-FC with the visual network's left calcarine cortex (**Table 7**; **Figure 9**), with no significant PCC rs-FC correlation observed. As raised in the previous discussion section, the calcarine cortex exhibits altered baseline connectivity and sensory-gating deficits in trauma-exposed populations (Harnett et al., 2025). Within the defence cascade model, the vlPAG promotes emotional over-modulation via the parasympathetic "brake," which dampens the integration of environmental sensory stimuli, whereas the dlPAG drives sympathetic reactivity and emotional under-modulation (Harricharan et al., 2016; Lanius et al., 2010b; Mobbs et al., 2007). Speculatively, this pre-to-post NFB correlation between alpha modulation and increased vlPAG-calcarine cortex rs-FC may suggest a mechanistic shift. Following NFB, successful alpha modulation may remediate sensory gating deficits, allowing individuals with PTSD to more adaptively integrate/regulate environmental sensory stimuli (Clancy et al., 2020b).

4.4 Fourth hypothesis: correlations with clinical scores

Regarding the multiple regression analyses of clinical scores, our fourth hypothesis was supported. Greater reductions in PTSD severity (CAPS 1-2 scores) in the experimental group correlated with decreased dlPAG rs-FC with the lPCC using the *a priori* PCC ROI (**Table 7**; **Figure 9**). Here, the PCC was selected as an *a priori* target based on recent evidence that the PAG's defensive survival systems disrupt normal DMN cortical connectivity in PTSD, serving as a primary neural mechanism for the fragmentation of self-experience often seen in traumatized individuals (Terpou et al., 2020). Our findings expand on this model by demonstrating that alpha-desynchronizing EEG-NFB can actively down-regulate this pathologically elevated hyperarousal pathway. Specifically, down-regulating the subcortical IAS—represented here by the dlPAG—may alleviate persistent clinical symptoms of hypervigilance (Webb et al., 2020; Zhang et al., 2024). Concurrently, decoupling this alarm system from the lPCC—a core hub of the DMN—may liberate the node from constant threat-related hijacking (Terpou et al., 2019a, 2020; Lanius et al., 2020). This dual mechanism would support both an enhanced, coherent sense of self at rest and a diminished vulnerability to threat-induced identity fragmentation. Consequently, this novel result suggests that NFB can reduce pathologically elevated rs-FC between a central node of the IAS and a midline cortical structure dedicated to self-referential processing.

Furthermore, lower dissociation severity scores (MDI 2) post-NFB in the experimental group were associated with increased lPCC rs-FC with the right mid/anterior insula (**Table 7**; **Figure 9**). Interestingly, Bluhm and colleagues (2009) found reduced rs-FC between the PCC and the right insula in participants with PTSD compared to healthy controls. The mid insula is important for a sense of body ownership and movement awareness, integrating distinct bodily feelings associated with emotionally salient environmental stimuli (Nicholson et al., 2016b; Craig, 2009). The anterior insula is vital for self-awareness, interoception, and cognitive control, with the right anterior insula regulating sympathetic activity (Tegeler et al., 2014). The dissociative subtype of PTSD is characterized by decreased activation and disrupted functional connectivity of the anterior insula (Harricharan et al., 2020; Lanius et al., 2010b). This blunted insular response correlates directly with the severity of depersonalization and derealization symptoms, serving as a neural marker of the profound bodily detachment and emotional overmodulation unique to dissociation (Nicholson et al., 2016b; Sierra & David, 2011). Furthermore, the anterior insula, as part of the SN with the amygdala and dorsal ACC (dACC), acts as a critical neuro-switch between task-focused CEN and self-referential DMN (Uddin et al., 2015, 2017). Akiki et al. (2017) found that an overactive SN in PTSD fails to modulate

these network dynamics, resulting in a hypoactive DMN at rest. Consequently, these novel results could suggest that post-NFB, the anterior insula within the SN has an increased capacity to modulate between the CEN and DMN as dissociative symptoms decrease.

Taken together, these clinical multiple regression results provide compelling, multi-network evidence for a neuroplastic shift in rs-FC patterns of individuals with PTSD following alpha-desynchronizing EEG-NFB. By coupling specific rs-FC changes with distinct clinical improvements, these data elucidate a dual mechanism of therapeutic recovery. On one hand, the post-NFB correlation between reduced PTSD symptom severity (CAPS) and decreased dlPAG–lPCC functional coupling demonstrates a direct downregulation of elevated subcortical-cortical defensive pathways. This specific decoupling effectively frees the DMN from constant, threat-related "hijacking" by the IAS, a phenomenon heavily implicated in trauma-induced hyperarousal and fragmented self-referential processing (Lanius et al., 2020; Terpou et al., 2020). In contrast, the distinct relationship between reduced dissociation symptom severity (MDI) and enhanced lPCC–mid/anterior insula connectivity marks a crucial restoration of somatic integration and cognitive flexibility.

5. Limitations and future directions

The findings of this study should be interpreted in light of several constraints. First, four individuals per PTSD group met the criteria for the dissociative subtype, which introduced heterogeneity to our sample as it is both functionally and clinically distinguishable from the non-subtype (Harricharan et al., 2016). Second, this study was not sufficiently powered to detect between-group differences or group-by-timepoint interactions. Therefore, our results are limited to PTSD participant and healthy control between-group baseline differences and within-group differences in the experimental and sham-control groups. We included a sham group to control for non-specific effects, including expectation and therapeutic contact. However, our small sample size lacks the statistical power to rule these factors out completely. Consequently, our results suggest, but do not establish, a specific treatment effect for NFB. Larger studies are needed to confirm whether the within-group changes observed here are truly treatment-specific.

Third, this study only examined resting-state data, not threat-stimulus data, limiting opportunities to assess differences in functional connectivity between the PAG and DMN during threat-stimulus paradigms at baseline or post-NFB. PAG functional connectivity alterations with DMN regions were previously found during threat-stimulus paradigms in PTSD (Terpou et al., 2019b, 2020). As such, future directions could include exploring potential

changes in functional connectivity of the PAG and DMN regions pre- to post-NFB using threat-stimulus paradigms in addition to resting-state.

Fourth, the data analyzed in this study did not include qualitative or quantitative questions regarding the sense of self at rest or under threat. Additionally, no quantitative or qualitative questions were administered to test whether participants with PTSD notice any changes in their ways of relating to their environment and others following treatment. As a result, we could not explore whether there were any associations among a participant's sense of self, their ways of relating to their environment and the functional connectivity patterns observed in the PAG and PCC at baseline or post-NFB. As well, including assessments of predictive processing of neutral stimuli at baseline and post-NFB would allow testing of whether EEG-NFB improves such processing in individuals with PTSD.

6. Conclusion

This study provides preliminary evidence that EEG-NFB may modulate key neural circuits implicated in PTSD, specifically by restoring PCC connectivity within the DMN while reducing hyperconnectivity between the PAG and IAS, associated with hypervigilance and arousal. These findings advance our understanding of PTSD neurobiology by providing direct evidence that targeted NFB can alter dysfunctional brain networks underlying core symptoms. This neurobiologically driven approach differs from traditional therapies by focusing on the restoration of healthy brain function, potentially offering a novel adjunctive treatment for PTSD. The observed alignment between neural changes and symptom reduction underscores the clinical relevance of these neural targets. While these results are preliminary and require validation in larger, diverse samples, they highlight the promise of EEG-NFB as a personalized intervention that could be integrated into future treatment protocols for PTSD. These findings offer hope for developing more targeted, brain-based interventions for individuals living with PTSD, potentially improving outcomes for those who do not respond to existing treatments.

Use of AI (artificial intelligence) assisted language tools

The author used Grammarly to assist with editing and final revisions of the document. The author fully reviewed, verified, and approved the core arguments, data analysis, and final phrasing.

Acknowledgment

This NFB trial was funded by the Canadian Institute for Veteran Health Research (CIMVHR; grant agreement No. W7716-125624/001/SV) and ANS Research, London, United

Kingdom. SueEllen MacGowan has received funding support from the National Legion Foundation's Masters Scholarship, Canada Graduate Scholarship – Masters (Canadian Institutes of Health Research), University of Ottawa Entrance Scholarship, the University of Ottawa's Institute of Mental Health Research at the Royal's Genevieve MacKinnon Award and a stipend from the Atlas Institute for Veterans and Families. We are also thankful to Suzy Southwell, Barbara Whelan, and Stephanie Nevil for contributing to data collection and curation.

References

Abdallah, C. G., Southwick, S. M., & Krystal, J. H. (2017). Neurobiology of posttraumatic stress disorder (PTSD): A path from novel pathophysiology to innovative therapeutics. *Neuroscience Letters*, 649, 130–132. https://doi.org/10.1016/j.neulet.2017.04.046

Adolphs, R. (2009). The social brain: Neural basis of social knowledge. *Annual Review of Psychology, 60*, 693–716. https://doi.org/10.1146/annurev.psych.60.110707.163514

Adolphs, R., Baron-Cohen, S., & Tranel, D. (2002). Impaired recognition of social emotions following amygdala damage. *Journal of Cognitive Neuroscience, 14*(8), 1264–1274. https://doi.org/10.1162/089892902760807258

American Psychiatric Association. (2022). *Diagnostic and statistical manual of mental disorders: DSM-5-TR* (5th ed.). American Psychiatric Association Publishing.

Akiki, T. J., Averill, C. L., & Abdallah, C. G. (2017). A network-based neurobiological model of PTSD: Evidence from structural and functional neuroimaging studies. *Current Psychiatry Reports,* 19(11), 81. https://doi.org/10.1007/s11920-017-0840-4

Akiki, T. J., Averill, C. L., Wrocklage, K. M., Scott, J. C., Averill, L. A., Schweinsburg, B., Alexander-Bloch, A., Martini, B., Southwick, S. M., Krystal, J. H., & Abdallah, C. G. (2018). Default mode network abnormalities in posttraumatic stress disorder: A novel network-restricted topology approach. *NeuroImage, 176*, 489–498. https://doi.org/10.1016/j.neuroimage.2018.05.005

Andrews-Hanna, J. R., Reidler, J. S., Sepulcre, J., Poulin, R., & Buckner, R. L. (2010). Functional-anatomic fractionation of the brain's default network. *Neuron, 65*(4), 550–562. https://doi.org/10.1016/j.neuron.2010.02.005

Arnaldo, I., Corcoran, A. W., Friston, K. J., & Ramstead, M. J. D. (2022). Stress and its sequelae: An active inference account of the etiological pathway from allostatic overload to depression. *Neuroscience and Biobehavioral Reviews, 135*, 104590. https://doi.org/10.1016/j.neubiorev.2022.104590

Azarias, F. R., Almeida, G. H. D. R., de Melo, L. F., Rici, R. E. G., & Maria, D. A. (2025). The Journey of the Default Mode Network: Development, Function, and Impact on Mental Health. *Biology, 14*(4), 395. https://doi.org/10.3390/biology14040395

Bandler, R., Keay, K. A., Floyd, N., & Price, J. (2000). Central circuits mediating patterned autonomic activity during active vs. passive emotional coping. *Brain Research Bulletin, 53*(1), 95–104. https://doi.org/10.1016/S0361-9230(00)00313-0

Bao, W., Gao, Y., Cao, L., Li, H., Liu, J., Liang, K., Hu, X., Zhang, L., Hu, X., Gong, Q., & Huang, X. (2021). Alterations in large-scale functional networks in adult posttraumatic stress disorder: A systematic review and meta-analysis of resting-state functional connectivity studies. *Neuroscience and Biobehavioral Reviews, 131*, 1027–1036. https://doi.org/10.1016/j.neubiorev.2021.10.017

Benarroch, E. E. (2012). Periaqueductal gray: An interface for behavioral control. *Neurology, 78*(3), 210–217. https://doi.org/10.1212/WNL.0b013e31823fcdee

Blake, D. D., Weathers, F. W., Nagy, L. M., Kaloupek, D. G., Gusman, F. D., Charney, D. S., & Keane, T. M. (1995). The development of a clinician-administered PTSD scale. *Journal of Traumatic Stress 8*(1), 75–90. https://doi.org/10.1002/jts.2490080106

Blanke, O., Slater, M., & Serino, A. (2015). Behavioral, neural, and computational principles of bodily self-consciousness. *Neuron, 88*(1), 145–166. https://doi.org/10.1016/j.neuron.2015.09.029

Bluhm, R. L., Williamson, P. C., Osuch, E. A., Frewen, P. A., Stevens, T. K., Boksman, K., Neufeld, R. W. J., Théberge, J., & Lanius, R. A. (2009). Alterations in default network connectivity in posttraumatic stress disorder related to early-life trauma. *Journal of Psychiatry & Neuroscience, 34*(3), 187–194. https://doi.org/10.1139/jpn.0925

Bowman, A. D., Griffis, J. C., Visscher, K. M., Dobbins, A. C., Gawne, T. J., DiFrancesco, M. W., & Szaflarski, J. P. (2017). Relationship between alpha rhythm and the default mode network: An EEG-fMRI study. *Journal of Clinical Neurophysiology, 34*(6), 527–533. https://doi.org/10.1097/WNP.0000000000000411

Brewin, C. R. (2011). The nature and significance of memory disturbance in posttraumatic stress disorder. Annual Review of *Clinical Psychology, 7*, 203–227. https://doi.org/10.1146/annurev-clinpsy-032210-104544

Brewin, C. R. (2014). Episodic memory, perceptual memory, and their interaction: Foundations for a theory of posttraumatic stress disorder. *Psychological Bulletin*, *140*(1), 69–97. https://doi.org/10.1037/a0033722

Brinkmann, L., Buff, C., Neumeister, P., Tupak, S. v., Becker, M. P. I., Herrmann, M. J., & Straube, T. (2017). Dissociation between amygdala and bed nucleus of the stria terminalis during threat anticipation in female post-traumatic stress disorder patients. *Human Brain Mapping*, *38*(4), 2190–2205. https://doi.org/10.1002/hbm.23513

Buckner, R. L., Andrews-Hanna, J. R., & Schacter, D. L. (2008). The brain's default network: Anatomy, function, and relevance to disease. *Annals of the New York Academy of Sciences, 1124*, 1–38. https://doi.org/10.1196/annals.1440.011

Cavanna, A. E., & Trimble, M. R. (2006). The precuneus: A review of its functional anatomy and behavioural correlates. *Brain, 129*(3), 564–583. https://doi.org/10.1093/brain/awl004

Clancy, K. J., Albizu, A., Schmidt, N. B., & Li, W. (2020a). Intrinsic sensory disinhibition contributes to intrusive re-experiencing in combat veterans. *Scientific Reports, 10*(1), 963. https://doi.org/10.1038/s41598-020-57963-2

Clancy, K. J., Andrzejewski, J. A., Simon, J., Ding, M., Schmidt, N. B., & Li, W. (2020b). Posttraumatic stress disorder is associated with a dysrhythmia across the visual cortex and the default mode network. *ENeuro*, *7*(4), e0053-20.2020. https://doi.org/10.1523/ENEURO.0053-20.2020

Clancy, K., Ding, M., Bernat, E., Schmidt, N. B., & Li, W. (2017). Restless "rest": Intrinsic sensory hyperactivity and disinhibition in post-traumatic stress disorder. *Brain*, *140*(7), 2041–2050. https://doi.org/10.1093/brain/awx116

Corrigan, F. M., & Christie-Sands, J. (2020). An innate brainstem self-other system involving orienting, affective responding, and polyvalent relational seeking: Some clinical implications for a “Deep Brain Reorienting” trauma psychotherapy approach. *Medical Hypotheses, 136*, 109502. https://doi.org/10.1016/j.mehy.2019.109502

Craig, A. D. (2009). How do you feel — now? The anterior insula and human awareness. *Nature Reviews Neuroscience*, *10*, 59–70. https://doi.org/10.1038/nrn2555

de Lange, F. P., Heilbron, M., & Kok, P. (2018). How do expectations shape perception? *Trends in Cognitive Sciences, 22*(9), 764–779. https://doi.org/10.1016/j.tics.2018.06.002

Diedrichsen, J. (2006). A spatially unbiased atlas template of the human cerebellum. *NeuroImage*, *33*(1), 127–138. https://doi.org/10.1016/j.neuroimage.2006.05.056

Diedrichsen, J., Balsters, J. H., Flavell, J., Cussans, E., & Ramnani, N. (2009). A probabilistic MR atlas of the human cerebellum. *NeuroImage*, *46*(1), 39–46. https://doi.org/10.1016/j.neuroimage.2009.01.045

DiGangi, J. A., Tadayyon, A., Fitzgerald, D. A., Rabinak, C. A., Kennedy, A., Klumpp, H., Rauch, S. A. M., & Phan, K. L. (2016). Reduced default mode network connectivity following combat trauma. *Neuroscience Letters, 615*, 37–43. https://doi.org/10.1016/j.neulet.2016.01.010

du Bois, N., Bigirimana, A. D., Korik, A., Kéthina, L. G., Rutembesa, E., Mutabaruka, J., Mutesa, L., Prasad, G., Jansen, S., & Coyle, D. H. (2021). Neurofeedback with low-cost, wearable electroencephalography (EEG) reduces symptoms in chronic post-traumatic stress disorder. *Journal of Affective Disorders*, *295*, 1319–1334. https://doi.org/10.1016/j.jad.2021.08.071

Eisenberg, M. L., Rodebaugh, T. L., Flores, S., & Zacks, J. M. (2023). Impaired prediction of ongoing events in posttraumatic stress disorder. *Neuropsychologia*, *188*, 108636. https://doi.org/10.1016/j.neuropsychologia.2023.108636

Enten, L. K., DeMarco, A., Kline, R., Globisch, F. M., Dunsmoor, J. E., Cisler, J. M., Nemeroff, C. B., & Fonzo, G. A. (2025). Altered amygdala and striatal responsivity and prediction error encoding of temporal reward dynamics in post-trauma psychopathology. *Neuropsychopharmacology, 51*(5), 904–915. https://doi.org/10.1038/s41386-025-02276-z

Ergenoglu, T., Demiralp, T., Bayraktaroglu, Z., Ergen, M., Beydagi, H., & Uresin, Y. (2004). Alpha rhythm of the EEG modulates visual detection performance in humans. *Cognitive Brain Research, 20*(3), 376–383. https://doi.org/10.1016/j.cogbrainres.2004.03.009

Ezra, M., Faull, O. K., Jbabdi, S., & Pattinson, K. T. S. (2015). Connectivity-based segmentation of the periaqueductal gray matter in human with brainstem optimized diffusion MRI. *Human Brain Mapping, 36*(9), 3459–3471. https://doi.org/10.1002/hbm.22855

First, M. B., Spitzer, R. L., Gibbon, M., & Williams, J. B. W. (2002). *Structured Clinical Interview for DSM-IV-TR Axis I Disorders, Patient Edition (SCID-I/P, 11/2002 revision)*. Biometrics Research, New York State Psychiatric Institute.

Foster, B. L., Koslov, S. R., Aponik-Gremillion, L., Monko, M. E., Hayden, B. Y., & Heilbronner, S. R. (2023). A tripartite view of the posterior cingulate cortex. *Nature Reviews Neuroscience, 24*, 173–189. https://doi.org/10.1038/s41583-022-00661-x

Fisher, S. F. (2014). *Neurofeedback in the treatment of developmental trauma: Calming the fear-driven brain.* W. W. Norton & Company.

Fox, M. D., & Greicius, M. (2010). Clinical applications of resting state functional connectivity. *Frontiers in Systems Neuroscience, 4*, 19. https://doi.org/10.3389/fnsys.2010.00019

Fransson, P. (2005). Spontaneous low-frequency BOLD signal fluctuations: An fMRI investigation of the resting-state default mode of brain function hypothesis. *Human Brain Mapping, 26*, 15–29. https://doi.org/10.1002/hbm.20113

Friston, K. (2010). The free-energy principle: a unified brain theory? *Nature Reviews Neuroscience, 11*(2), 127–138. https://doi.org/10.1038/nrn2787

Friston, K. J., & Frith, C. D. (2015). Active inference, communication and hermeneutics. *Cortex*, *68*, 129–143. https://doi.org/10.1016/j.cortex.2015.03.025

Friston, K., Mattout, J., & Kilner, J. (2011). Action understanding and active inference. *Biological Cybernetics*, *104*(1–2), 137–160. https://doi.org/10.1007/s00422-011-0424-z

Halvorsen, J. Ø. (2016). Defining clinically significant change. *The British Journal of Psychiatry, 209*(1), 85. https://doi.org/10.1192/bjp.209.1.85

Harnett, N. G., Rowland, G. E., Webb, E. K., Li, T., Joshi, S., Ressler, K. J., & Rosso, I. M. (2025). Traumatic stress alters neural reactivity to visual stimulation. *Digital Psychiatry and Neuroscience*, *3*(1), 9. https://doi.org/10.1038/s44277-025-00030-3

Harricharan, S., Nicholson, A. A., Thome, J., Densmore, M., McKinnon, M. C., Théberge, J., Frewen, P. A., Neufeld, R. W. J., & Lanius, R. A. (2020). PTSD and its dissociative subtype through the lens of the insula: Anterior and posterior insula resting-state functional connectivity and its predictive validity using machine learning. *Psychophysiology, 57*(1), e13472. https://doi.org/10.1111/psyp.13472

Harricharan, S., Rabellino, D., Frewen, P. A., Densmore, M., Théberge, J., McKinnon, M. C., Schore, A. N., & Lanius, R. A. (2016). fMRI functional connectivity of the periaqueductal gray in PTSD and its dissociative subtype. *Brain and Behavior, 6*(12), e00579. https://doi.org/10.1002/brb3.579

Jensen, O., & Mazaheri, A. (2010). Shaping functional architecture by oscillatory alpha activity: Gating by inhibition. *Frontiers in Human Neuroscience*, *4*, 186. https://doi.org/10.3389/fnhum.2010.00186

Kanwisher, N., Mcdermott, J., & Chun, M. M. (1997). The fusiform face area: A module in human extrastriate cortex specialized for face perception. *The Journal of Neuroscience*, *17*(11), 4302–4311. https://doi.org/10.1523/JNEUROSCI.17-11-04302.1997

Kearney, B. E., & Lanius, R. A. (2022). The brain-body disconnect: A somatic sensory basis for trauma-related disorders. *Frontiers in Neuroscience, 16*, 1015749. https://doi.org/10.3389/fnins.2022.1015749

Kearney, B. E., & Lanius, R. A. (2024). Why reliving is not remembering and the unique neurobiological representation of traumatic memory. *Nature Mental Health 2*(10), 1142-1151. https://doi.org/10.1038/s44220-024-00324-z

King, A. P., Block, S. R., Sripada, R. K., Rauch, S., Giardino, N., Favorite, T., Angstadt, M., Kessler, D., Welsh, R., & Liberzon, I. (2016). Altered default mode network (DMN) resting state functional connectivity following a mindfulness-based exposure therapy for posttraumatic stress disorder (PTSD) in combat veterans of Afghanistan and Iraq. *Depression and Anxiety*, *33*(4), 289–299. https://doi.org/10.1002/da.22481

Klimesch, W. (2012). α-band oscillations, attention, and controlled access to stored information. *Trends in Cognitive Sciences, 16*(12), 606–617. https://doi.org/10.1016/j.tics.2012.10.007

Kluetsch, R. C., Ros, T., Théberge, J., Frewen, P. A., Calhoun, V. D., Schmahl, C., Jetly, R., & Lanius, R. A. (2014). Plastic modulation of PTSD resting-state networks and subjective wellbeing by EEG neurofeedback. *Acta Psychiatrica Scandinavica*, *130*(2), 123–136. https://doi.org/10.1111/acps.12229

Koch, S. B. J., van Zuiden, M., Nawijn, L., Frijling, J. L., Veltman, D. J. & Olff, M. (2016). Aberrant resting-state brain activity in posttraumatic stress disorder: A meta-analysis and systematic review. *Depression and Anxiety, 33*(7), 592–605. https://doi.org/10.1002/da.22478

Kozlowska, K., Walker, P., McLean, L., & Carrive, P. (2015). Fear and the defense cascade: Clinical implications and management. *Harvard Review of Psychiatry, 23*(4), 263–287. https://doi.org/10.1097/HRP.0000000000000065

Lanius, R. A., Bluhm, R. L., Coupland, N. J., Hegadoren, K. M., Rowe, B., Théberge, J., Neufeld, R. W. J., Williamson, P. C., & Brimson, M. (2010a). Default mode network connectivity as a predictor of post-traumatic stress disorder symptom severity in acutely traumatized subjects. *Acta Psychiatrica Scandinavica*, *121*(1), 33–40. https://doi.org/10.1111/j.1600-0447.2009.01391.x

Lanius, R. A., Boyd, J. E., McKinnon, M. C., Nicholson, A. A., Frewen, P., Vermetten, E., Jetly, R., & Spiegel, D. (2018). A review of the neurobiological basis of trauma-related dissociation and its relation to cannabinoid- and opioid-mediated stress response: A transdiagnostic, translational approach. *Current Psychiatry Reports, 20*(12), 118. https://doi.org/10.1007/s11920-018-0983-y

Lanius, R. A., Harricharan, S., Kearney, B. E., & Pandev-Girard, B. (2025). *Sensory pathways to healing from trauma: Harnessing the brain's capacity for change.* Guilford Press.

Lanius, R. A., Rabellino, D., Boyd, J. E., Harricharan, S., Frewen, P. A., & McKinnon, M. C. (2017). The innate alarm system in PTSD: conscious and subconscious processing of threat. *Current Opinion in Psychology*, *14*, 109–115. https://doi.org/10.1016/j.copsyc.2016.11.006

Lanius, R. A., Terpou, B. A., & McKinnon, M. C. (2020). The sense of self in the aftermath of trauma: lessons from the default mode network in posttraumatic stress disorder. *European Journal of Psychotraumatology*, *11*(1). https://doi.org/10.1080/20008198.2020.1807703

Lanius, R. A., Vermetten, E., Loewenstein, R. J., Brand, B., Christian, S., Bremner, J. D., & Spiegel, D. (2010b). Emotion modulation in PTSD: Clinical and neurobiological evidence for a dissociative subtype. *American Journal of Psychiatry, 167*(6), 640–647. https://doi.org/10.1176/appi.ajp.2009.09081168

Lanius, R. A., Williamson, P. C., Bluhm, R. L., Densmore, M., Boksman, K., Neufeld, R. W. J., Gati, J. S., & Menon, R. S. (2005). Functional connectivity of dissociative responses in posttraumatic stress disorder: A functional magnetic resonance imaging investigation. *Biological Psychiatry, 57*(8), 873–884. https://doi.org/10.1016/j.biopsych.2005.01.011

Leech, R., & Sharp, D. J. (2014). The role of the posterior cingulate cortex in cognition and disease. *Brain, 137*(1), 12–32. https://doi.org/10.1093/brain/awt162

Leech, R., Kamourieh, S., Beckmann, C. F., & Sharp, D. J. (2011). Fractionating the default mode network: Distinct contributions of the ventral and dorsal posterior cingulate cortex to cognitive control. *Journal of Neuroscience, 31*(9), 3217–3224. https://doi.org/10.1523/JNEUROSCI.5626-10.2011

Liberzon, I., & Abelson, J. L. (2016). Context Processing and the Neurobiology of Post-Traumatic Stress Disorder. *Neuron, 92*(1), 14–30. https://doi.org/10.1016/j.neuron.2016.09.039

Lieberman, J. M., Rabellino, D., Densmore, M., Frewen, P. A., Steyrl, D., Scharnowski, F., Théberge, J., Hosseini-Kamkar, N., Neufeld, R. W. J., Jetly, R., Frey, B. N., Ros, T., Lanius, R. A., & Nicholson, A. A. (2023a). A tale of two targets: examining the differential effects of posterior cingulate cortex- and amygdala-targeted fMRI-neurofeedback in a PTSD pilot study. *Frontiers in Neuroscience*, *17*. https://doi.org/10.3389/fnins.2023.1229729

Lieberman, J. M., Brady, B., Lanius, R. A., Ros, T., Théberge, J., Frey, B. N., Bhat, V., Scharnowski, F., & Nicholson, A. A. (2026). Longitudinal mapping of a randomized controlled trial of EEG neurofeedback in PTSD: Early symptom stabilization and implications for adjunctive therapeutic potential. *Psychiatry Research - Neuroimaging*, *361*. https://doi.org/10.1016/j.pscychresns.2026.112244

Lieberman, J. M., Rabellino, D., Densmore, M., Frewen, P. A., Steyrl, D., Scharnowski, F., Théberge, J., Neufeld, R. W. J., Schmahl, C., Jetly, R., Narikuzhy, S., Lanius, R. A., & Nicholson, A. A. (2023b). Posterior cingulate cortex targeted real-time fMRI neurofeedback recalibrates functional connectivity with the amygdala, posterior

insula, and default-mode network in PTSD. *Brain and Behavior*, *13*(3). https://doi.org/10.1002/brb3.2883

Linson, A., Parr, T., & Friston, K. J. (2020). Active inference, stressors, and psychological trauma: A neuroethological model of (mal)adaptive explore-exploit dynamics in ecological context. *Behavioural Brain Research*, *380*. https://doi.org/10.1016/j.bbr.2019.112421

Lokshina, Y., Nickelsen, T., & Liberzon, I. (2021). Reward Processing and Circuit Dysregulation in Posttraumatic Stress Disorder. *Frontiers in Psychiatry*, *12*. https://doi.org/10.3389/fpsyt.2021.559401

Maldjian, J. A., Laurienti, P. J., Kraft, R. A., & Burdette, J. H. (2003). An automated method for neuroanatomic and cytoarchitectonic atlas-based interrogation of fmri data sets. *NeuroImage, 19*, 1233–1239. https://doi.org/10.1016/S1053-8119(03)00169-1.

Meadows, M. E. (2011). Calcarine Cortex. In J. S. Kreutzer, J. DeLuca, & B. Caplan (Eds.), *Encyclopedia of Clinical Neuropsychology.* (pp. 472). Springer. https://doi.org/10.1007/978-0-387-79948-3_1348

Menon, V. (2011). Large-scale brain networks and psychopathology: A unifying triple network model. *Trends in Cognitive* Sciences, 15(10), 483–506. https://doi.org/10.1016/j.tics.2011.08.003

Miller, D. R., Hayes, S. M., Hayes, J. P., Spielberg, J. M., Lafleche, G., & Verfaellie, M. (2017). Default mode network subsystems are differentially disrupted in posttraumatic stress disorder. *Biological Psychiatry: Cognitive Neuroscience and Neuroimaging*, *2*(4), 363–371. https://doi.org/10.1016/j.bpsc.2016.12.006

Miller, E. K., & Cohen, J. D. (2001). An integrative theory of prefrontal cortex function. *Annual Review of Neuroscience, 24*(1), 167-202. https://doi.org/10.1146/annurev.neuro.24.1.167

Mobbs, D., Petrovic, P., Marchant, J. L., Hassabis, D., Weiskopf, N., Seymour, B., Dolan, R. J., & Frith, C. D. (2007). When fear is near: Threat imminence elicits prefrontal-periaqueductal gray shifts in humans. *Science*, *317*(5841), 1079–1083. https://doi.org/10.1126/science.1144298

Nicholson, A. A., Densmore, M., Frewen, P. A., Neufeld, R. W. J., Théberge, J., Jetly, R., Lanius, R. A., & Ros, T. (2023). Homeostatic normalization of alpha brain rhythms within the default-mode network and reduced symptoms in post-traumatic stress disorder following a randomized controlled trial of electroencephalogram neurofeedback. *Brain communications, 5*(2). https://doi.org/10.1093/braincomms/fcad068

Nicholson, A. A., Friston, K. J., Zeidman, P., Harricharan, S., McKinnon, M. C., Densmore, M., Neufeld, R. W. J., Théberge, J., Corrigan, F., Jetly, R., Spiegel, D., & Lanius, R. A. (2017). Dynamic causal modeling in PTSD and its dissociative subtype: Bottom–up versus top–down processing within fear and emotion regulation circuitry. *Human Brain Mapping*, *38*(11), 5551–5561. https://doi.org/10.1002/hbm.23748

Nicholson, A. A., Harricharan, S., Densmore, M., Neufeld, R. W. J., Ros, T., McKinnon, M. C., Frewen, P. A., Théberge, J., Jetly, R., Pedlar, D., & Lanius, R. A. (2020a). Classifying heterogeneous presentations of PTSD via the default mode, central executive, and salience networks with machine learning. *NeuroImage: Clinical*, *27*. https://doi.org/10.1016/j.nicl.2020.102262

Nicholson, A. A., Ros, T., Densmore, M., Frewen, P. A., Neufeld, R. W. J., Théberge, J., Jetly, R., & Lanius, R. A. (2020b). A randomized, controlled trial of alpha-rhythm EEG neurofeedback in posttraumatic stress disorder: A preliminary investigation showing evidence of decreased PTSD symptoms and restored default mode and salience network connectivity using fMRI. *NeuroImage: Clinical*, *28*. https://doi.org/10.1016/j.nicl.2020.102490

Nicholson, A. A., Ros, T., Frewen, P. A., Densmore, M., Théberge, J., Kluetsch, R. C., Jetly, R., & Lanius, R. A. (2016a). Alpha oscillation neurofeedback modulates amygdala complex connectivity and arousal in posttraumatic stress disorder. *NeuroImage: Clinical*, *12*, 506–516. https://doi.org/10.1016/j.nicl.2016.07.006

Nicholson, A. A., Sapru, I., Densmore, M., Frewen, P. A., Neufeld, R. W. J., Théberge, J., McKinnon, M. C., & Lanius, R. A. (2016b). Unique insula subregion resting-state functional connectivity with amygdala complexes in posttraumatic stress disorder and its dissociative subtype. *Psychiatry Research: Neuroimaging*, *250*, 61–72. https://doi.org/10.1016/j.pscychresns.2016.02.002

Nolan, H., Whelan, R., & Reilly, R. B. (2010). FASTER: Fully Automated Statistical Thresholding for EEG artifact Rejection. *Journal of Neuroscience Methods, 192*(1), 152–162. https://doi.org/10.1016/j.jneumeth.2010.07.015

Northoff, G., & Bermpohl, F. (2004). Cortical midline structures and the self. *Trends in Cognitive Sciences*, *8*(3), 102–107. https://doi.org/10.1016/j.tics.2004.01.004

Olivé, I., Densmore, M., Harricharan, S., Théberge, J., McKinnon, M. C., & Lanius, R. (2018). Superior colliculus resting state networks in post-traumatic stress disorder and its dissociative subtype. *Human Brain Mapping*, *39*(1), 563–574. https://doi.org/10.1002/hbm.23865

Parr, T., & Friston, K. J. (2017). Working memory, attention, and salience in active inference. *Scientific Reports*, *7*(1). https://doi.org/10.1038/s41598-017-15249-0

Pearson, J., Naselaris, T., Holmes, E. A., & Kosslyn, S. M. (2015). Mental imagery: functional mechanisms and clinical applications. *Trends in Cognitive Sciences, 19*(10), 590–602. https://doi.org/10.1016/j.tics.2015.08.003

Peelen, M. v., & Downing, P. E. (2005). Selectivity for the human body in the fusiform gyrus. *Journal of Neurophysiology*, *93*(1), 603–608. https://doi.org/10.1152/jn.00513.2004

Putica, A., & Agathos, J. (2024). Reconceptualizing complex posttraumatic stress disorder: A predictive processing framework for mechanisms and intervention. *Neuroscience and Biobehavioral Reviews, 164.* https://doi.org/10.1016/j.neubiorev.2024.105836

Qin, L. di, Wang, Z., Sun, Y. W., Wan, J. Q., Su, S. S., Zhou, Y., & Xu, J. R. (2012). A preliminary study of alterations in default network connectivity in post-traumatic

stress disorder patients following recent trauma. Brain Research, 1484, 50–56. https://doi.org/10.1016/j.brainres.2012.09.029

Rabellino, D., Densmore, M., Harricharan, S., Jean, T., McKinnon, M. C., & Lanius, R. A. (2018a). Resting-state functional connectivity of the bed nucleus of the stria terminalis in post-traumatic stress disorder and its dissociative subtype. *Human Brain Mapping*, *39*(3), 1367–1379. https://doi.org/10.1002/hbm.23925

Rabellino, D., Densmore, M., Théberge, J., McKinnon, M. C., & Lanius, R. A. (2018b). The cerebellum after trauma: Resting-state functional connectivity of the cerebellum in posttraumatic stress disorder and its dissociative subtype. *Human brain mapping, 39*(8), 3354–3374. https://doi.org/10.1002/hbm.24081

Ros, T., Enriquez-Geppert, S., Zotev, V., Young, K. D., Wood, G., Whitfield-Gabrieli, S., Wan, F., Vuilleumier, P., Vialatte, F., van de Ville, D., Todder, D., Surmeli, T., Sulzer, J. S., Strehl, U., Sterman, M. B., Steiner, N. J., Sorger, B., Soekadar, S. R., Sitaram, R., … Thibault, R. T. (2020). Consensus on the reporting and experimental design of clinical and cognitive-behavioural neurofeedback studies (CRED-nf checklist). *Brain*, *143*(6), 1674–1685. https://doi.org/10.1093/brain/awaa009

Ros, T., Théberge, J., Frewen, P. A., Kluetsch, R., Densmore, M., Calhoun, V. D., & Lanius, R. A. (2013). Mind over chatter: Plastic up-regulation of the fMRI salience network directly after EEG neurofeedback. *NeuroImage*, *65*, 324–335. https://doi.org/10.1016/j.neuroimage.2012.09.046

Ros, T., Baars, B. J., Lanius, R. A., & Vuilleumier, P. (2014). Tuning pathological brain oscillations with neurofeedback: A systems neuroscience framework. *Frontiers in Human Neuroscience*, *8*(DEC). https://doi.org/10.3389/fnhum.2014.01008

Ross, M. C., & Cisler, J. M. (2020). Altered large-scale functional brain organization in posttraumatic stress disorder: A comprehensive review of univariate and network-level neurocircuitry models of PTSD. *Neuroimage: Clinical, 27*. https://doi.org/10.1016/j.nicl.2020.102319

Roy, M., Shohamy, D., Daw, N., Jepma, M., Wimmer, G. E., & Wager, T. D. (2014). Representation of aversive prediction errors in the human periaqueductal gray. *Nature Neuroscience*, *17*(11), 1607–1612. https://doi.org/10.1038/nn.3832

Saenger, V. M., Barrios, F. A., Martínez-Gudiño, M. L., & Alcauter, S. (2012). Hemispheric asymmetries of functional connectivity and grey matter volume in the default mode network. *Neuropsychologia, 50*(7), 1308–1315. https://doi.org/10.1016/j.neuropsychologia.2012.02.014

Scheinost, D., Stoica, T., Saksa, J., Papademetris, X., Constable, R.T., Pittenger, C., & Hampson, M. (2013). Orbitofrontal cortex neurofeedback produces lasting changes in contamination anxiety and resting-state connectivity. *Translational Psychiatry, 3*(4), e250. https://doi.org/10.1038/tp.2013.24

Shaw, S. B., Nicholson, A. A., Ros, T., Harricharan, S., Terpou, B., Densmore, M., Theberge, J., Frewen, P., & Lanius, R. A. (2023). Increased top-down control of emotions during symptom provocation working memory tasks following a RCT of alpha-down

neurofeedback in PTSD. *NeuroImage: Clinical*, *37*. https://doi.org/10.1016/j.nicl.2023.103313

Sierra, M., & David, A. S. (2011). Depersonalization: A selective impairment of self-awareness. *Consciousness and Cognition, 20*(1), 99-108. https://doi.org/10.1016/j.concog.2010.10.018

Siminski, N., Böhme, S., Zeller, J. B. M., Becker, M. P. I., Bruchmann, M., Hofmann, D., Breuer, F., Mühlberger, A., Schiele, M. A., Weber, H., Schartner, C., Deckert, J., Pauli, P., Reif, A., Domschke, K., Straube, T., & Herrmann, M. J. (2021). BNST and amygdala activation to threat: Effects of temporal predictability and threat mode. *Behavioural Brain Research*, *396*. https://doi.org/10.1016/j.bbr.2020.112883

Sitaram, R., Ros, T., Stoeckel, L., Haller, S., Scharnowski, F., Lewis-Peacock, J., Weiskopf, N., Blefari, M. L., Rana, M., Oblak, E., Birbaumer, N., & Sulzer, J. (2017). Closed-loop brain training: The science of neurofeedback. *Nature Reviews Neuroscience, 18*(2), 86–100. https://doi.org/10.1038/nrn.2016.164

Solms, M. (2022). *The hidden spring: A journey to the source of consciousness*. Norton paperback.

Sorger, B., Scharnowski, F., Linden, D. E. J., Hampson, M., & Young, K. D. (2019). Control freaks: Towards optimal selection of control conditions for fMRI neurofeedback studies. *NeuroImage, 186*, 256–265. https://doi.org/10.1016/j.neuroimage.2018.11.004

Somerville, L. H., Whalen, P. J., & Kelley, W. M. (2010). Human bed nucleus of the stria terminalis indexes hypervigilant threat monitoring. *Biological Psychiatry*, *68*(5), 416–424. https://doi.org/10.1016/j.biopsych.2010.04.002

Spreng, R. N., & Grady, C. L. (2009). Patterns of brain activity supporting autobiographical memory, prospection, and theory of mind, and their relationship to the default mode network. *Journal of Cognitive Neuroscience, 22*(6), 1112–1123. https://doi.org/10.1162/jocn.2009.21282

Sripada, R. K., King, A. P., Welsh, R. C., Garfinkel, S. N., Wang, X., Sripada, C. S., & Liberzon, I. (2012). Neural dysregulation in posttraumatic stress disorder: Evidence for disrupted equilibrium between salience and default mode brain networks. *Psychosomatic Medicine, 74*(9), 904–911. https://doi.org/10.1097/PSY.0b013e318273bf33

Steuwe, C., Daniels, J. K., Frewen, P. A., Densmore, M., Pannasch, S., Beblo, T., Reiss, J., & Lanius, R. A. (2014). Effect of direct eye contact in PTSD related to interpersonal trauma: An fMRI study of activation of an innate alarm system. *Social Cognitive and Affective Neuroscience, 9*(1), 88–97. https://doi.org/10.1093/scan/nss105

Stuss, D. T. (2011). Functions of the frontal lobes: Relation to executive functions. *Journal of the International Neuropsychological Society, 17*(5), 759-765. https://doi.org/10.1017/S1355617711000695

Sutin, A.R., & Robins, R.W. (2007). Phenomenology of autobiographical memories: The memory experiences questionnaire. *Memory, 15*(4), 390–411. https://doi.org/10.1080/09658210701256654

Tanaka, S., & Kirino, E. (2021). The precuneus contributes to embodied scene construction for singing in an opera. *Frontiers in Human Neuroscience, 15*. https://doi.org/10.3389/fnhum.2021.737742

Tegeler, C. H., Lee, S. W., & Shaltout, H. A. (2014). Significance of right anterior insula activity for mental health intervention. *JAMA Psychiatry*, *71*(3), 336. https://doi.org/10.1001/jamapsychiatry.2013.3507

Terpou, B. A., Densmore, M., Théberge, J., Frewen, P., McKinnon, M. C., Nicholson, A. A., & Lanius, R. A. (2020). The hijacked self: Disrupted functional connectivity between the periaqueductal gray and the default mode network in posttraumatic stress disorder using dynamic causal modeling. *NeuroImage: Clinical, 27*. https://doi.org/10.1016/j.nicl.2020.102345

Terpou, B. A., Densmore, M., Théberge, J., Thome, J., Frewen, P., McKinnon, M. C., & Lanius, R. A. (2019a). The threatful self: midbrain functional connectivity to cortical midline and parietal regions during subliminal trauma-related processing in PTSD. *Chronic Stress, 3*. https://doi.org/10.1177/2470547019871369

Terpou, B. A., Densmore, M., Thome, J., Frewen, P., McKinnon, M. C., & Lanius, R. A. (2019b). The innate alarm system and subliminal threat presentation in posttraumatic stress disorder: Neuroimaging of the Midbrain and Cerebellum. *Chronic Stress*, *3*. https://doi.org/10.1177/2470547018821496

Terpou, B. A., Harricharan, S., McKinnon, M. C., Frewen, P., Jetly, R., & Lanius, R. A. (2019c). The effects of trauma on brain and body: A unifying role for the midbrain periaqueductal gray. *Journal of Neuroscience Research, 97*(9), 1110–1140. https://doi.org/10.1002/jnr.24447

Thome, J., Densmore, M., Frewen, P. A., McKinnon, M. C., Théberge, J., Nicholson, A. A., Koenig, J., Thayer, J. F., & Lanius, R. A. (2017). Desynchronization of autonomic response and central autonomic network connectivity in posttraumatic stress disorder. *Human Brain Mapping*, 38(1), 27–40. https://doi.org/10.1002/hbm.23340

Uddin, L. Q. (2015). *Salience processing and insular cortical function and dysfunction*. Nature Reviews Neuroscience 16(1), 55–61. https://doi.org/10.1038/nrn3857

Uddin, L. Q., Nomi, J. S., Hébert-Seropian, B., Ghaziri, J., & Boucher, O. (2017). Structure and Function of the Human Insula. *Journal of Clinical Neurophysiology, 34*(4), 300–306. https://doi.org/10.1097/WNP.0000000000000377

Utevsky, A.V., Smith, D.V., & Huettel, S.A. (2014). Precuneus is a functional core of the default-mode network. *Journal of Neuroscience, 34*(3), 932–940. https://doi.org/10.1523/JNEUROSCI.4227-13.2014

Vianna, D. M. L., Graeff, F. G., Landeira-Fernandez, J., & Brandão, M. L. (2001). Lesion of the ventral periaqueductal gray reduces conditioned fear but does not change freezing induced by stimulation of the dorsal periaqueductal gray. *Learning and Memory, 8*(3), 164–169. https://doi.org/10.1101/lm.36101

Viard, A., Mutlu, J., Chanraud, S., Guenolé, F., Egler, P. J., Gérardin, P., Baleyte, J. M., Dayan, J., Eustache, F., & Guillery-Girard, B. (2019). Altered default mode network connectivity in adolescents with post-traumatic stress disorder. *NeuroImage: Clinical, 22*. 101731. https://doi.org/10.1016/j.nicl.2019.101731

Wandell, B. A., Dumoulin, S. O., & Brewer, A. A. (2007). Visual field maps in human cortex. *Neuron, 56*(2), 366–383. https://doi.org/10.1016/j.neuron.2007.10.012

Wang, Y., Guo, N., Zhao, L., Huang, H., Yao, X., Sang, N., Hou, X., Mao, Y., Bi, T., & Qiu, J. (2017). The structural and functional correlates of the efficiency in fearful face detection. *Neuropsychologia*, *100*, 1–9. https://doi.org/10.1016/j.neuropsychologia.2017.04.004

Walker, D. L., Toufexis, D. J., & Davis, M. (2003). Role of the bed nucleus of the stria terminalis versus the amygdala in fear, stress, and anxiety. *European Journal of Pharmacology*, *463*(1–3), 199–216. https://doi.org/10.1016/S0014-2999(03)01282-2

Weathers, F. W., Blake, D. D., Schnurr, P. P., Kaloupek, D. G., Marx, B. P., & Keane, T. M. (2013a). The clinician-administered PTSD scale for DSM-5 (CAPS-5). Interview available from the National Center for PTSD at www.ptsd.va.gov.

Weathers, F. W., Blake, D. D., Schnurr, P. P., Kaloupek, D. G., Marx, B. P., & Keane, T. M. (2013b). The life events checklist for DSM-5 (LEC-5). Instrument available from the National Center for PTSD at www.ptsd.va.gov

Webb, E. K., Huggins, A. A., Belleau, E. L., Taubitz, L. E., Hanson, J. L., deRoon-Cassini, T. A., & Larson, C. L. (2020). Acute post-trauma resting-state functional connectivity of periaqueductal gray prospectively predicts posttraumatic stress disorder symptoms. *Biological Psychiatry: Cognitive Neuroscience and Neuroimaging*, *5*(9), 891–900. https://doi.org/10.1016/j.bpsc.2020.03.004

Whitfield-Gabrieli, S., & Ford, J. M. (2012). Default mode network activity and connectivity in psychopathology. *Annual Review of Clinical Psychology, 8*, 49–76. https://doi.org/10.1146/annurev-clinpsy-032511-143049

Wolf, E. J., Lunney, C. A., Miller, M. W., Resick, P. A., Friedman, M. J., & Schnurr, P. P. (2012a). The dissociative subtype of PTSD: A replication and extension. *Depression and Anxiety*, *29*(8), 679–688. https://doi.org/10.1002/da.21946

Wolf, E. J., Miller, M. W., Reardon, A. F., Ryabchenko, K. A., Castillo, D., & Freund, R. (2012b). A Latent Class Analysis of Dissociation and Posttraumatic Stress Disorder: Evidence for a Dissociative Subtype. *Archives of General Psychiatry, 69*(7), 698–705. https://doi.org/10.1001/archgenpsychiatry.2011.1574

Xiao, S., Yang, Z., Su, T., Gong, J., Huang, L., & Wang, Y. (2022). Functional and structural brain abnormalities in posttraumatic stress disorder: A multimodal meta-analysis of neuroimaging studies. *Journal of Psychiatric Research, 155*, 153–162. https://doi.org/10.1016/j.jpsychires.2022.08.010

Yehuda, R., Hoge, C. W., McFarlane, A. C., Vermetten, E., Lanius, R. A., Nievergelt, C. M., Hobfoll, S. E., Koenen, K. C., Neylan, T. C., & Hyman, S. E. (2015). Post-traumatic

stress disorder. *Nature Reviews Disease Primers, 1*, 15057. https://doi.org/10.1038/nrdp.2015.57

Zhang, H., Zhu, Z., Ma, W. X., Kong, L. X., Yuan, P. C., Bu, L. F., Han, J., Huang, Z. L., & Wang, Y. Q. (2024). The contribution of periaqueductal gray in the regulation of physiological and pathological behaviors. *Frontiers in Neuroscience, 18*, 1380171. https://doi.org/10.3389/fnins.2024.1380171